



Cite this: *RSC Sustainability*, 2025, **3**, 1303

## Advanced catalytic strategies for CO<sub>2</sub> to methanol conversion: noble metal-based heterogeneous and electrochemical approaches

Soumalya Roy,<sup>af</sup> Ezhava Manu Manohar,<sup>a</sup> Sujoy Bandyopadhyay,<sup>b</sup> Manik Chandra Singh,<sup>c</sup> Yeji Cha,<sup>f</sup> Soumen Giri, <sup>\*d</sup> Sharad Lande, <sup>\*e</sup> Kyungsu Na, <sup>\*f</sup> Junseong Lee and Sourav Das <sup>\*a</sup>

The next generation is threatened by climate change, the significant impacts of global warming, and an energy crisis. Atmospheric CO<sub>2</sub> levels have surpassed the critical 400 ppm threshold due to significant reliance on fossil fuels to satisfy the increasing energy demands of our fast-progressing society. An overabundance of manufactured carbon dioxide (CO<sub>2</sub>) emissions severely disrupts the ecology. The synthesis of methanol by the selective hydrogenation of CO<sub>2</sub> is a viable approach for generating clean energy and sustainably safeguarding our biosphere. Methanol is a versatile molecule with several uses in the chemical industry as an alternative to fossil fuels. The methanol economy is recognized as a pivotal development in the pursuit of a net zero-emission fuel, representing a crucial stride toward a more sustainable planet. The developing green methanol industry, or renewable methanol initiative, primarily relies on CO<sub>2</sub> adsorption and usage. This novel technique is essential for mitigating global warming. This review focuses on the synthesis of methanol utilizing noble metal-based catalysts and electrochemical reduction methods, examining the associated thermodynamic challenges and outlining future directions for research. It emphasizes the role of noble metals, including palladium, gold, silver, and rhodium, in enhancing catalytic activity and selectivity during the CO<sub>2</sub> to methanol conversion process. The incorporation of these sophisticated catalytic processes improves methanol production efficiency and facilitates novel methods for carbon capture and usage, therefore advancing a more sustainable energy framework.

Received 29th November 2024  
Accepted 23rd January 2025

DOI: 10.1039/d4su00749b

rsc.li/rscsus



### Sustainability spotlight

A perspective on noble metal-based catalytic conversion of CO<sub>2</sub> to methanol through heterogeneous and electrochemical approaches presents a promising solution to address the increasing concerns regarding climate change. The current situation is critical: CO<sub>2</sub> emissions from industrial activities constitute a significant contributor to global warming, and elucidating efficient methods for converting CO<sub>2</sub> into valuable products is crucial for achieving sustainable development. Noble metal catalysts play a pivotal role in enhancing the selectivity, efficiency, and stability of CO<sub>2</sub> reduction reactions. The sustainable advancement of this research lies in optimizing these catalysts to facilitate CO<sub>2</sub> conversion at reduced energy inputs, thereby rendering the process more cost-effective and scalable for industrial applications. This research aligns with SDG 7 (Affordable and Clean Energy) by enabling the production of methanol as a clean fuel, SDG 9 (Industry, Innovation, and Infrastructure) through the development of advanced catalytic technologies, and SDG 13 (Climate Action) by addressing the reduction of CO<sub>2</sub> emissions and advancing climate solutions.

<sup>a</sup>Department of Basic Sciences, Chemistry Discipline, Institute of Infrastructure Technology Research And Management, Near Khokhra Circle, Maninagar East, Ahmedabad, 380026, Gujarat, India. E-mail: souravdas@iitram.ac.in; d.sourav245@gmail.com

<sup>b</sup>Department of Chemistry, Research Institute for Convergence of Basic Science and Research Institute for Natural Sciences, Hanyang University, Seoul 04763, Republic of Korea

<sup>c</sup>Dept. of Physics, Balarampur P. C. H. S School, Rangadih, Purulia, West Bengal, 723143, India

<sup>d</sup>School of Applied Sciences, Kalinga Institute of Industrial Technology, Bhubaneswar 751024, India. E-mail: giri.soumen02@gmail.com

<sup>e</sup>Research & Development, Reliance Industries Ltd, Thane Belapur Road, Ghansoli, Navi Mumbai, 400701, India. E-mail: sharad.lande@ril.com

<sup>f</sup>Department of Chemistry, Chonnam National University, 77 Yongbong-ro, Buk-gu, Gwangju 61186, Republic of Korea. E-mail: leespy@chonnam.ac.kr; kyungsu\_na@chonnam.ac.kr

## 1. Introduction

The use of fossil fuels has ushered in an era of extraordinary wealth and improved living standards for humanity.<sup>1,2</sup> However, excessive fossil fuel burning for energy generation elevates the emission of anthropogenic greenhouse gases (GHGs), mostly in the form of pollutant CO<sub>2</sub>. According to the International Energy Agency (IEA), Global Energy & CO<sub>2</sub> Status Report, in 2022 the worldwide CO<sub>2</sub> emissions will have peaked at about 36.8 Gt a new all-time high, and the current concentration of atmospheric CO<sub>2</sub> is approximately 421 ppm, which has increased by 50% since the beginning of the industrial age.<sup>3</sup> The massive release of CO<sub>2</sub> to the environment disrupts the Earth's natural

carbon cycle and global ecology, leading to substantial and feasibly irreversible changes in the world's climate such as global warming, ocean acidification, and sea level rise, which have a direct consequence on human health.<sup>4-7</sup> Green carbon science is the study and optimization of effective carbon resource processing, utilization, and recycling for lowering CO<sub>2</sub> emissions, lessening the greenhouse effect, reducing reliance on fossil fuels, and lowering the global carbon footprint.<sup>8-13</sup> Therefore, the creation of clean energy technology is the only option for the next generation.<sup>14-20</sup> In that sense, one of the main research focuses in energy engineering is the regulation and utilization of CO<sub>2</sub>.<sup>21-29</sup> In fact, recent years have seen the development of carbon capture and storage (CCS) technologies, which separate CO<sub>2</sub> from combustion byproducts or chemical processes for subsequent recycling or storage.<sup>30-35</sup> Direct capture of CO<sub>2</sub> from the atmosphere has garnered scientific and practical attention in recent times.<sup>36-46</sup> Despite reducing CO<sub>2</sub> emissions to a certain degree, CCS is not a viable long-term solution due to its exorbitant expense and the possibility of leakage.<sup>47-53</sup> Internationally, there are currently 20 active large-scale carbon capture and storage (CCS) facilities that annually separate around 40 million metric tons of carbon dioxide (CO<sub>2</sub>) and store it underground<sup>54-60</sup> (The Global Status of CCS; (Global CCS Institute: 2020)). However, this amount represents only 0.1% of the total global carbon emissions. However, the majority of these CCS projects fall under the category of enhanced oil recovery (EOR), which involves injecting CO<sub>2</sub> underground to assist in extracting fossil fuels with the aim of creating a financially viable business model.<sup>61-63</sup> The price for CO<sub>2</sub> sequestration from a power plant ranges from \$60 to \$100

per metric ton of CO<sub>2</sub>, excluding storage and transportation expenses.<sup>64-68</sup> Therefore, the implementation of EOR is essential to ensure the economic feasibility of CCS, which in turn leads to the introduction of more fossil fuels into the carbon cycle.<sup>69-73</sup> For CCS to have a significant influence on climate change, it must be commercialized through the development of cost-effective and energy-efficient systems.<sup>74-82</sup> Systems must ensure that the cost of producing CO<sub>2</sub>, regulated by authorities, exceeds the cost of capturing and storing it. This will help create an artificial carbon cycle. Additionally, we need to turn CO<sub>2</sub> into chemicals and fuels that are in high demand (Fig. 1).<sup>83,84</sup> This will serve to effectively utilize a significant portion of the surplus global CO<sub>2</sub>. Currently, around 230 million tons (Mt) of carbon dioxide (CO<sub>2</sub>) are utilized annually, as reported by the IEA in 2019.<sup>85,86</sup> However, CO<sub>2</sub> usage represents less than 1% of overall CO<sub>2</sub> emissions.<sup>87,88</sup> Currently, the market size limits the conversion of CO<sub>2</sub> into chemicals. Thus, the catalytic hydrogenation of CO<sub>2</sub> into value-added products is a key method for CO<sub>2</sub> utilization, leading to the production of carbon-based substances such as methanol, dimethyl ether, formaldehyde, urea and various hydrocarbons.<sup>89-95</sup> Among the products stated above, methanol (CH<sub>3</sub>OH) is a significant chemical feedstock that can be utilized as an alternative chemical for fossil fuels in internal combustion engines, fuel cells, and the production of formaldehyde, methyl-*tert*-butyl ether (MTBE), acetic acid, alkyl halides, etc.<sup>96-98</sup> According to the well-accepted hypothesis of Olah in a book titled "Beyond Oil and Gas: The Methanol Economy," methanol may be indispensable in the near future, and CO<sub>2</sub> hydrogenation is one of the most promising and regenerative routes for methanol synthesis.<sup>99</sup> The elevated

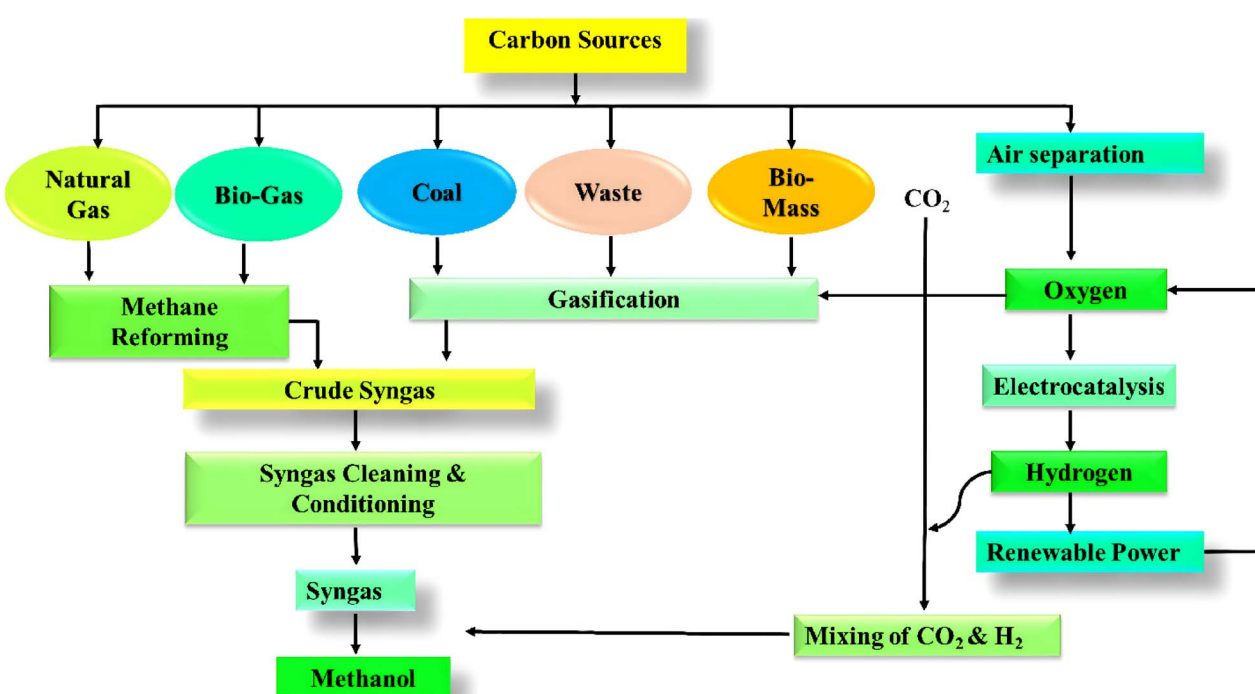


Fig. 1 Overview of key methanol synthesis methods using diverse carbon sources.



volumetric energy density of methanol renders it a feasible substitute for gasoline in internal combustion engines (ICEs), enhancing the octane rating. Moreover, in comparison to traditional gasoline internal combustion engines, methanol internal combustion engines produce markedly lower emissions of contaminants. The Indian government has been actively encouraging the adoption of clean transportation and the use of fuel-cell vehicles.<sup>100</sup> In 2012, the Dor Group initiated pilot testing following the decision by the Israeli government to explore alternative methods of reducing dependence on traditional fuels. One of the most promising approaches identified was the utilization of methanol as a substitute for petrol or as a component in petrol blends for internal combustion engines (Dor Group, 2019). China is also rapidly advancing the development of the methanol fuel market.

It is crucial to note that the hydrogen generated *via* water electrolysis can function as a long-term storage solution and be directly transferred to required locations for usage as a transportation fuel or in industrial applications. Moreover, hydrogen can be converted into electrofuels following the power-to-X concept, thereby storing renewable electrical energy within the chemical bonds of gaseous or liquid fuels.<sup>101,102</sup> Methanol can function as a carbon-neutral electrofuel when synthesized from hydrogen *via* electrolysis and carbon dioxide sourced from atmospheric capture, biomass, or industrial emissions<sup>103,104</sup> (Fig. 2). Methanol is a prominent and extensively traded chemical commodity, with the global methanol market projected to expand at a compound annual growth rate (CAGR) of 4.50% from 2022 to 2028.<sup>105,106</sup> In the chemical industry, methanol is used as both a feedstock and an energy carrier. Its applications range from organic transformations to sustainable

energy solutions, highlighting its importance in both traditional and emerging chemical processes. Methanol can function as a C1 source to facilitate various C–C and C–N bond formations and dehydrogenative coupling reactions, which are significant in the realms of natural product synthesis and drug development.<sup>107,108</sup> For instance, methanol is crucial for the production of formaldehyde, methylamine, methyl halides, methyl ethers, methyl esters, dimethyl ether, and acetic acid. It is additionally used in the manufacture of pharmaceuticals, biomolecules, agrochemicals, and polymers. Methanol may be transformed into olefins such as ethylene and propylene, which serve as essential building blocks for the petrochemical industry.<sup>109,110</sup> Furthermore, methanol serves as a versatile compound with applications as a solvent and/or additive in diverse industries, including paint removal, windshield washing fluids, and as a fermentation substrate in microbial production processes.<sup>111</sup>

In this context, it is noteworthy to mention that homogeneous (organometallic catalysts, metal-free catalysts, and N-heterocyclic carbenes) and heterogeneous catalyst systems have recently been successfully developed, and they are excellent candidates for hydrogenation of CO<sub>2</sub> to produce methanol.<sup>112–123</sup> Another highly appealing strategy extensively studied by the scientific community is the direct electrocatalytic carbon dioxide reduction reaction (ECO<sub>2</sub>RR).<sup>124–126</sup> In this instance, the term “direct ECO<sub>2</sub>RR” denotes the complete conversion of CO<sub>2</sub> to a specific product, methanol, at a single electrode.<sup>127–129</sup> In electrocatalytic technology, customized catalysts can improve electrode interface reaction kinetics.<sup>130,131</sup> It lowers activation energy and helps electrolyte reactants move electrons.<sup>132,133</sup> Electrocatalysts accelerate electron transit from

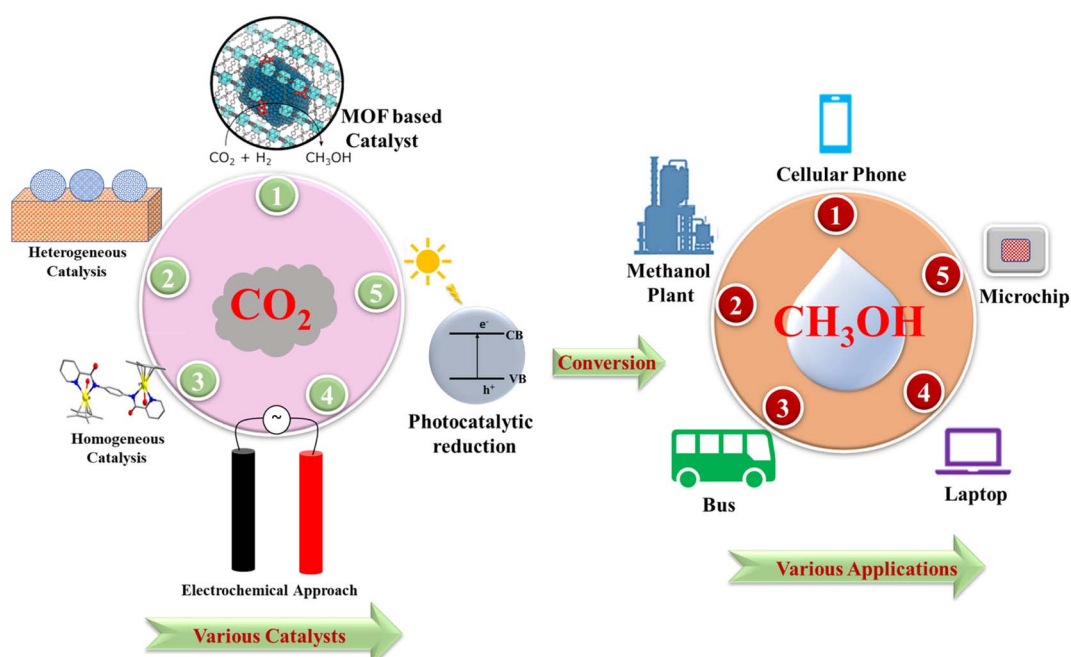


Fig. 2 Various approaches for converting CO<sub>2</sub> to CH<sub>3</sub>OH.



noble metals to other materials by lowering voltage.<sup>134–138</sup> To improve performance, researchers strive to augment the number of active sites and elevate the intrinsic activity of these sites. This involves fine-tuning the electronic and structural properties of the active sites to improve their catalytic efficiency.<sup>139</sup> Recent methodologies exploit local electrostatic fields to enhance the adhesion of electrode surfaces for intermediates, facilitating proton transfer to electron-rich active species and enabling the electrochemical reduction of CO<sub>2</sub> to produce methane.<sup>140</sup> In another study, Zhou *et al.* reported the O-philic adsorption strategy to facilitate the electrosynthesis of urea.<sup>141</sup> This study enhances our comprehension of how to control the properties of reactant adsorption–desorption dynamics for targeted conversion pathways within a comprehensive reactive multistep process pertinent to diverse electrocatalytic applications.

The first commercial methanol production unit was established in Anyang, Henan Province, China. Here methanol was synthesized using the waste carbon dioxide and hydrogen gases.<sup>142</sup> This process used the Emissions-to-Liquids (ETL) technology which was initiated by Carbon Recycling International (CRI) and the first pilot plant was established in Iceland.<sup>143</sup> Another emerging technology in the methanol economy is the CAMRE process, jointly developed by the Korea Institute of Science and Technology and POSCO.<sup>144</sup> Carbon Recycling International developed a pilot plant for the commercial synthesis of methanol from CO<sub>2</sub>. In this, the source of CO<sub>2</sub> is the Orka geothermal power plant and hydrogen is generated from the electrolysis of water from the Icelandic power grid and the methanol production capacity is 4000 tons per year. Blue Fuel Energy (BFE) is Canadian Methanol Corporation's conventional methanol production unit which produces methanol and gasoline based on the MTG process. Emerging techniques for producing methanol from CO<sub>2</sub> include photocatalytic conversion, electrochemical reduction, photoelectrochemical reduction, chemical conversion and plasma reactor technologies.<sup>145–154</sup>

A large number of metal-based catalysts have been employed for methanol synthesis, but the most popular catalyst in CO<sub>2</sub>-derived methanol synthesis is Cu/ZnO/Al<sub>2</sub>O<sub>3</sub>.<sup>23,155–161</sup> The major drawback of Cu based catalysts is their pyrophoric properties and low stability arising from sintering and agglomeration enhanced by the generation of water and mobility of ZnO.<sup>156,162–165</sup> This review focuses on the synthesis of CH<sub>3</sub>OH from the hydrogenation of CO<sub>2</sub> by employing noble metal based heterogeneous catalysts. The main advantages of noble metal-based catalysts are their excellent stability and resistance to the sintering effect, making them alternatives to Cu-based catalysts.<sup>166–170</sup> An efficient heterogeneous catalyst possesses moderate binding strength with the reactant and intermediate.<sup>171–174</sup> The success of catalytic reactions depends on the identification of the active site, accompanied by an understanding of structure–activity relationships that derive catalytic descriptors to explain the catalysis.<sup>175–179</sup> Current research emphasizes that noble metal-based catalysts are superior for the conversion of CO<sub>2</sub> to CO *via* the so-called reverse water gas-shift (RWGS) reaction with high reaction rates and high selectivity.<sup>180–184</sup> Noble metal catalysts are

excellent for CO<sub>2</sub> hydrogenation due to their unique electronic and structural properties, specifically their unique tunable d-band centers.<sup>185–190</sup> The d-band center mainly represents the energy level of the d-electrons relative to the Fermi level, strongly influencing the adsorption and activation of reactants such as CO<sub>2</sub> and H<sub>2</sub>.<sup>191–193</sup> The alignment of the d band center with the Fermi level enhanced the catalytic activity by optimizing the binding strength of intermediates.<sup>194,195</sup> Pd exhibits an intermediate d band center, effectively balancing CO<sub>2</sub> activation and methanol desorption.<sup>158,196</sup> In contrast, Au with a lower d band center reduces the strong binding of intermediates, which enhances selectivity. Experimental evidence suggests that Pd based catalysts show high turnover frequencies (TOFs) and methanol selectivity compared to non-noble metals owing to their superior activation energies and adsorption energies.<sup>197–199</sup> So, the manipulation of d band centers enhances the catalytic performance by tailoring the adsorption energies.<sup>200–202</sup> It has been a widely accepted strategy to manipulate the<sup>203</sup> d-band center of noble metals integrated with other metal compounds such as metal oxides/hydroxides and carbides by the electronic effect, which influenced the interface of atomic rearrangement with the geometric effect and strain effect.<sup>204</sup> The catalytic reaction mainly occurs at the interface such as the metal–metal interface, metal–porous material interface or metal–metal oxides/hydroxides/carbides interface which leads to enhanced the catalytic activity of hydrogenation of CO<sub>2</sub>.<sup>205,206</sup> The synthesis strategy of noble metal based heterogeneous catalysts with a proper understanding of structure–property relationships such as the active site of the catalyst, morphology, composition, strain, metal support interaction, crystallinity, defects *etc.* is one of the great achievements of the energy engineering sector.<sup>185,207,208</sup> A promising strategy should be adopted for utilizing noble metal-based catalysts. In this respect, the strategy of incorporating bulk metals into nanostructure supported catalysts boosts the cost-effective industrial production of methanol.

Recently, several excellent reviews have been published and paved the way to catalytic CO<sub>2</sub> conversion to value-added chemicals.<sup>209–214</sup> However, the main aim of this comprehensive review is the hydrogenation of CO<sub>2</sub> to CH<sub>3</sub>OH using heterogeneous noble metal-based catalysts with an electrochemical approach. This review first focuses on the physical and chemical properties of CO<sub>2</sub> with thermodynamic considerations. Then we have briefly addressed various approaches to the catalytic conversion of CO<sub>2</sub> to CH<sub>3</sub>OH such as the homogeneous approach, heterogeneous approach, photocatalytic approach, and electrochemical conversion approach, summarizing the catalytic journey of CO<sub>2</sub> to CH<sub>3</sub>OH. The mechanism of the conversion of CO<sub>2</sub> to CH<sub>3</sub>OH is one of the interesting sides of this article. Then the progress of noble metal-based heterogeneous catalysts is deeply discussed with structure–property relationships. We also provide an overview of the electrochemical reduction approach for the conversion of CO<sub>2</sub> to CH<sub>3</sub>OH. The challenges and possibilities of CO<sub>2</sub> reduction for industrial applications are also included. Finally, we have included the future scope and perspectives of methanol synthesized from CO<sub>2</sub>.



## 2. Physicochemical nature and activation of CO<sub>2</sub>

A CO<sub>2</sub> molecule in its neutral state belongs to the  $D_{\infty b}$  point group and has a linear structure, with a bond length between carbon and oxygen of 1.17 Å. Because of the electronegativity differences, the net electronic structure of the molecule can be represented as O<sup>-δ</sup>-C<sup>+2δ</sup>-O<sup>-δ</sup>.<sup>215</sup> In light of this, bifunctional catalytic sites are required to activate the C-O bond in an efficient manner, as the C atom is electrophilic and the O atoms are nucleophilic.<sup>216</sup> The highest occupied molecular orbital (HOMO) of CO<sub>2</sub> is located on the more electronegative oxygen atoms, whereas the lowest unoccupied molecular orbital (LUMO) is composed of the hybrid orbitals. The reduction of carbon dioxide (CO<sub>2</sub>) introduces an electron into its LUMO. This results in the molecule undergoing a conformational shift to accommodate the energy differences between each orbital, thereby enhancing its ability to interact with nucleophiles. Simultaneously, the localized electron density of oxygen lone pairs allows the HOMO to interact with electrophiles. As a result, a meta-stable radical adduct (CO<sub>2</sub><sup>·-</sup>) is generated in a bent shape that is kinetically stable (an activation energy barrier of ~0.4 eV) with an average lifetime of 60–90 μs. The common metal center (metal oxide), which is usually used for CO<sub>2</sub> reduction, where CO<sub>2</sub> is physisorbed, exhibits several coordination modes, such as monodentate, bidentate, or even tridentate, depending on the surface atomic arrangement.<sup>217</sup>

## 3. Conversion of CO<sub>2</sub> to methanol: thermodynamic aspects

In the present era, syngas (CO and H<sub>2</sub> mixture) is one of the main resources for the commercial production of methanol. In methanol synthesis, the H/C ratio is crucial, so to balance this ratio, a small amount of CO<sub>2</sub>, *i.e.* 2–8% is added to the CO/H<sub>2</sub> mixture to enhance the reaction rate.<sup>218</sup>



Reverse water gas shift (RWGS) reaction:



The processes of making methanol from CO<sub>2</sub> hydrogenation and the RWGS reaction are limited by thermodynamics. As the reaction temperature increases, the CO<sub>2</sub> conversion rate drops. It is important to note that the synthesis of methanol from CO<sub>2</sub> is an exothermic process that competes with the RWGS reaction, an endothermic reaction. According to Le Chatelier's principle, high pressure and low temperature thermodynamically favor CO<sub>2</sub> conversion to methanol. But considering the chemical inertness of CO<sub>2</sub>, a higher temperature makes CO<sub>2</sub> activation easier for methanol production, but it can also lead to increased selectivity towards the undesirable RWGS reaction thermodynamically to produce CO and H<sub>2</sub>O. In this way, the RWGS process not only

consumes hydrogen but also lowers the CO<sub>2</sub> equilibrium conversion rate, hence reducing the generation of methanol.<sup>70</sup> It was observed that less than 40% methanol was obtained from CO<sub>2</sub> at 200 °C but at the aforesaid temperature, more than 80% yield was obtained from the syngas process. Therefore, high pressure and lower temperature are required to control the RWGS process<sup>219</sup> (Fig. 3). According to the reaction (eqn (1)), as compared to the syngas strategy, methanol synthesis from CO<sub>2</sub> hydrogenation requires an additional quantity of hydrogen for the removal of one oxygen atom from CO<sub>2</sub>, yielding water as a by-product (eqn (2)).<sup>220</sup> It is important to note that water, a byproduct of both processes, enhances catalyst sintering. This phenomenon deactivates the catalyst and reduces the efficiency of subsequent steps in methanol production.<sup>221</sup> Therefore, the foregoing explanation implies that thermodynamic equilibrium limits the maximum methanol yield; nevertheless, the equilibrium constraint on methanol yield may be bypassed by optimizing reaction conditions, activating the catalyst, using promoters, developing new reactor designs, *etc.*<sup>222,223</sup>

However, if we take into account the CO<sub>2</sub> thermodynamic potential, the following reduction reactions occur:

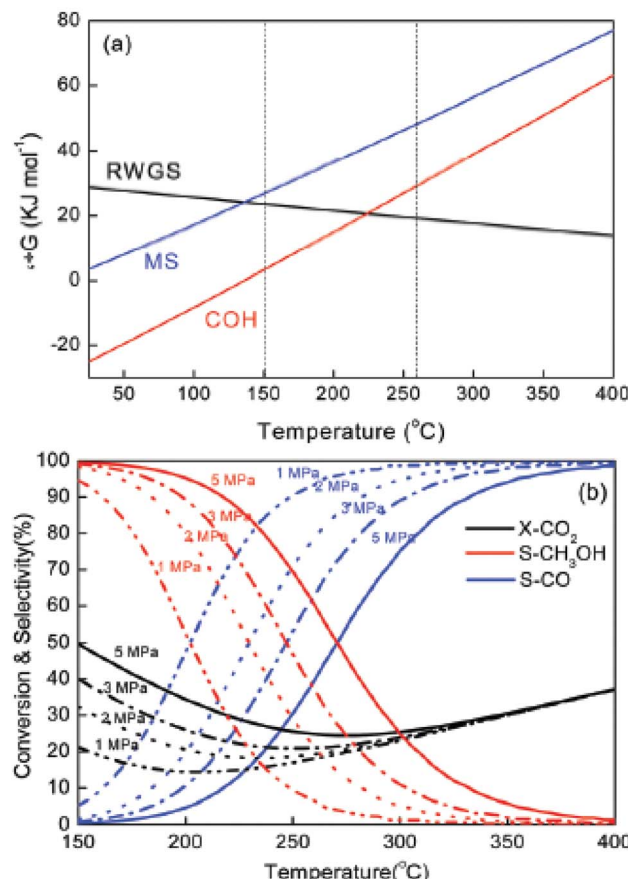
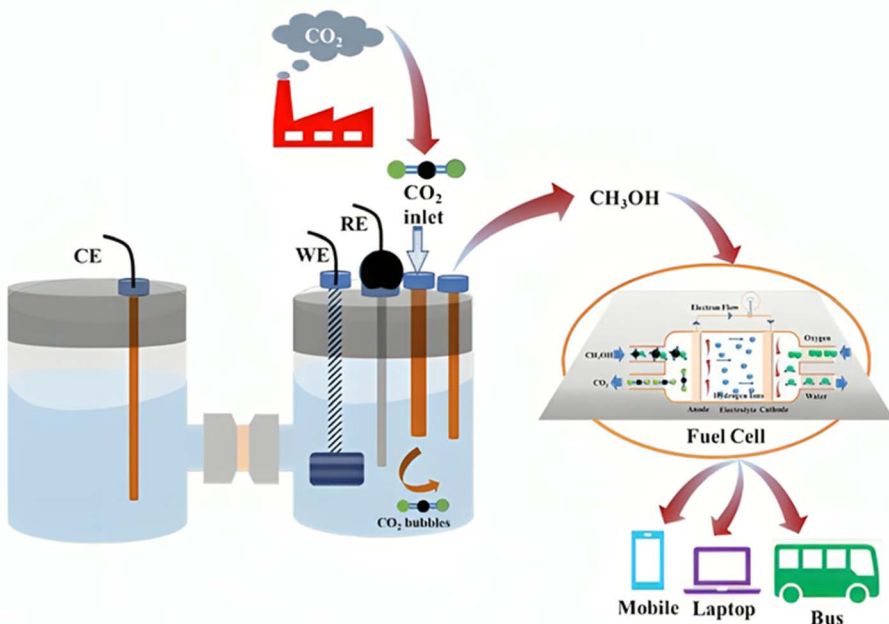
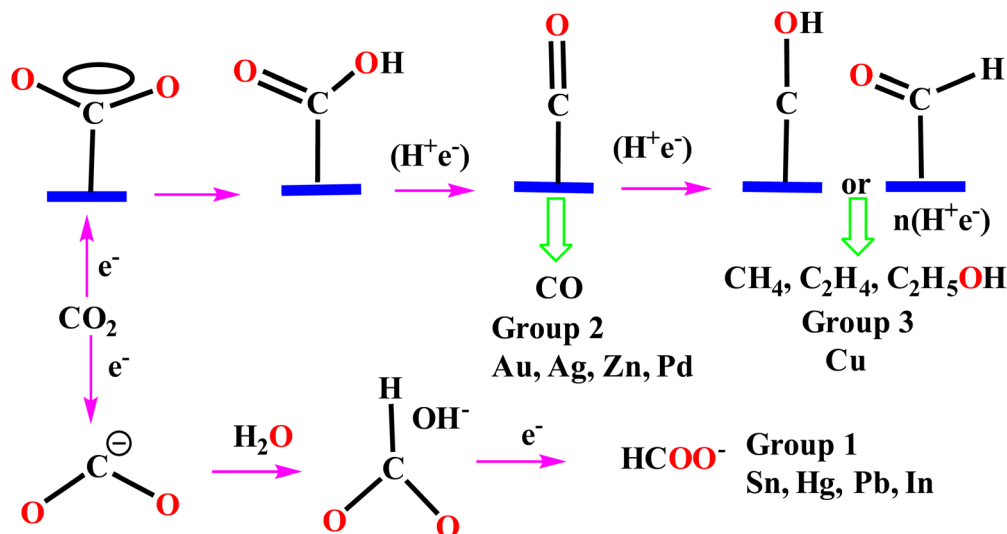
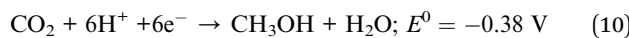
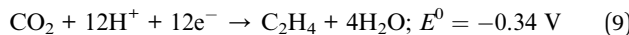
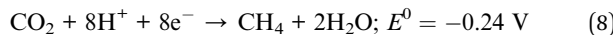
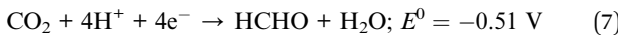
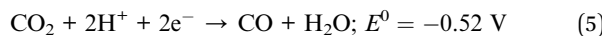
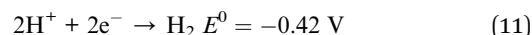
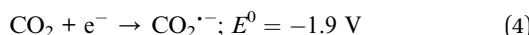
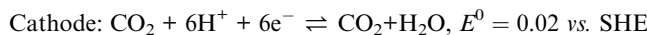


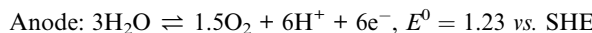
Fig. 3 (a) Free energy of methanol synthesis (MS) from CO<sub>2</sub>, RWGS and syngas hydrogenation (COH). (b) Equilibrium conversion-selectivity values of the CO<sub>2</sub>-hydrogenation reaction at various pressures. Reprinted with permission from ref. 156. Copyright 2020 Royal Society of Chemistry.



Fig. 4 Schematic representation of ECO<sub>2</sub>R to CH<sub>3</sub>OH.<sup>138</sup>Fig. 5 Reaction mechanism of the electrochemical CO<sub>2</sub>RR on metal electrodes in aqueous solutions.<sup>224</sup>

From the above reaction sequences, it can be observed that the overpotential of CO<sub>2</sub> is high (eqn (4)) and it's a multi-electron process. The CO<sub>2</sub> reduction is challenging as it generates the hydrogen evolution reaction (HER) if we compare it with the last two reactions. Again, for the CO<sub>2</sub> reduction reaction, the following processes are involved in the cathode (reduction) and anode (oxidation):





If we look at water splitting at 1.23 V vs. SHE and the overall  $\text{CO}_2$  reduction reaction, then a positive difference of only 20 mV exists. Therefore, a catalyst with a high hydrogen overpotential is preferred as it allows the carbon dioxide reduction reaction to achieve high selectivity and excellent rates before water reduction occurs, which is a process bottleneck (Fig. 4).

In order to be effective in  $\text{CO}_2$  reduction, noble-metal-based catalysts must be able to reduce the overpotential by which their activity is enhanced and able to show remarkable selectivity and stability. The below figure depicts the groupwise metal activity on  $\text{CO}_2$  reduction and the overall idea (Fig. 5).

## 4. Mechanism of $\text{CO}_2$ conversion to $\text{CH}_3\text{OH}$

The  $\text{CO}_2$  hydrogenation mechanism depends on various factors such as stability, activity and selectivity of the catalyst.<sup>157,225</sup>

According to the prevailing theory, the first step deals with the  $\text{CO}_2$  conversion to  $\text{CO}$ , which acts as a scavenger to eliminate the  $\text{H}_2\text{O}$  and the function of derived oxygen species is to inhibit active metal sites.<sup>226-228</sup> The use of isotope tracer tests has further supported the notion that  $\text{CO}_2$  serves as the elementary carbon source for the production of methanol from syngas or  $\text{CO}_2$  (ref. 229) (Fig. 6).

The theoretical and computational tools provide the validation of this reaction mechanism with experimental results. In this respect, DFT analysis, microkinetic modeling, and Monte Carlo simulation offer novel methods for developing  $\text{CO}_2$  hydrogenation catalysts.<sup>230-235</sup>

### 4.1 The HCOO mechanism

Researchers have followed the formate mechanistic path where  $\text{CO}_2$  interacts with formate ( $\text{HCOO}$ ) via the Eley–Rideal (ER) or Langmuir–Hinshelwood (LH) mechanism, and the reaction proceeds through  $\text{H}_2\text{COO}^*$ ,  $\text{H}_2\text{CO}^*$ , and  $\text{CH}_3\text{OH}$ .<sup>236-242</sup> The RWGS approach generates unstable  $\text{HCO}^*$  species which further dissociate into  $\text{CO}$  and  $\text{H}$ . Investigations using XPS, TPD, and IRAS techniques demonstrate that bidentate formate compounds play a crucial role in modifying the surface under

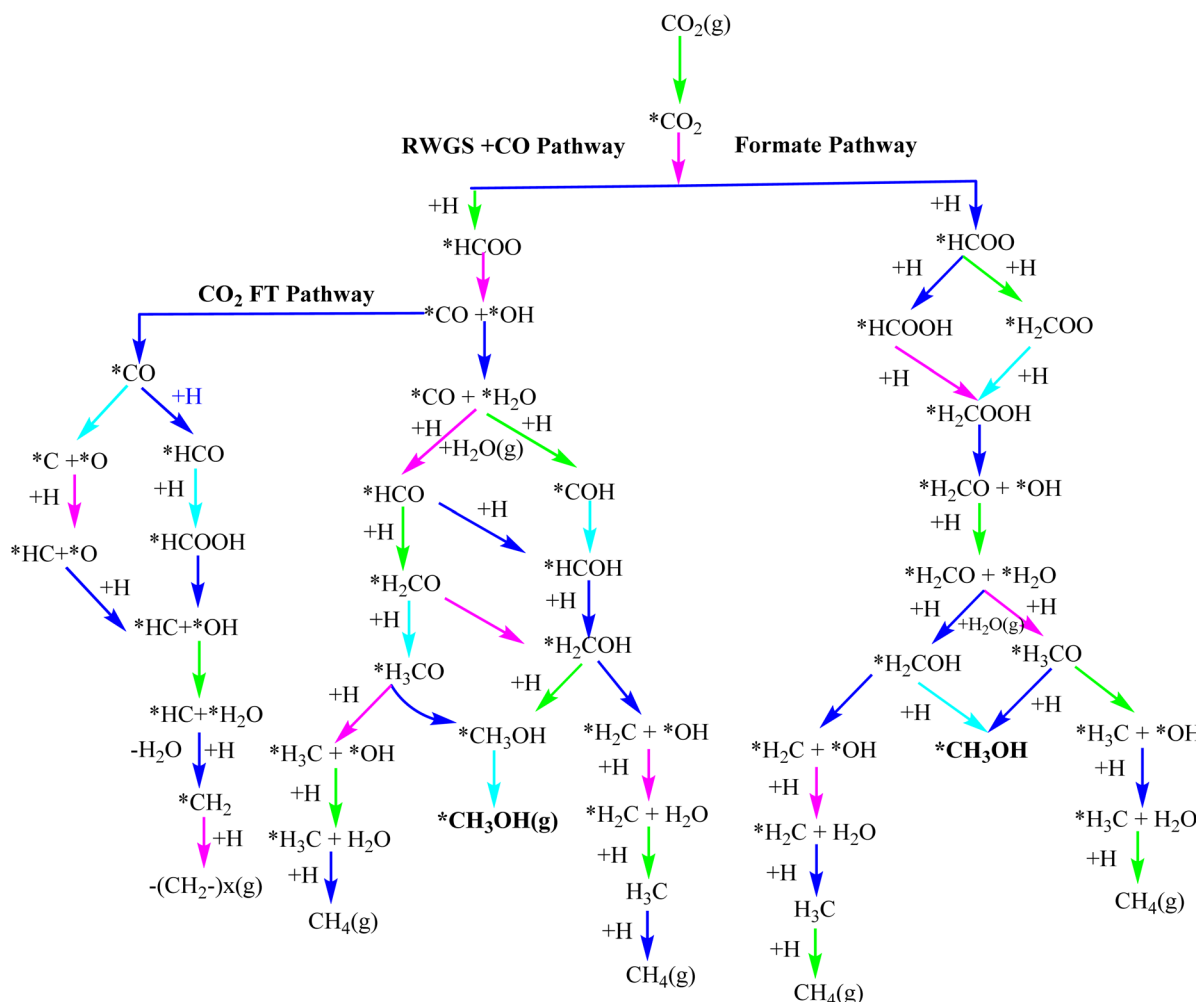


Fig. 6 Reaction mechanism of  $\text{CH}_3\text{OH}$  synthesis from  $\text{CO}_2$ .<sup>157</sup>



reaction conditions and serve as stable intermediates during the production of  $\text{CH}_3\text{OH}$ .<sup>243,244</sup> The methanol synthesis proceeds through the formate mechanistic pathway over Pd based catalysts Pd/ $\beta$ - $\text{Ga}_2\text{O}_3$ , Pd@Zn core shell catalyst, and Pd<sub>4</sub>/In<sub>2</sub>O<sub>3</sub>.<sup>231,245,246</sup>

In this mechanism, the C–O bond gets dissociated by the hydrogenation of  $\text{HCOO}^*/\text{H}_2\text{COO}^*$  and is the rate determining step of the reaction.<sup>247–249</sup> According to the microkinetic model, the rate determining step is the hydrogenation of  $\text{HCOO}$  to  $\text{H}_2\text{COO}$  on Pd– $\text{Ga}_2\text{O}_3$ /silica.<sup>250,251</sup>

#### 4.2 The revised HCOO mechanism

According to studies on a revised formate pathway,  $\text{HCOO}^*$  is hydrogenated to form  $\text{HCOOH}^*$ , which is then hydrogenated to form  $\text{H}_2\text{COOH}^*$  and dissociates to form  $\text{H}_2\text{CO}^*$  and OH.  $\text{H}_2\text{CO}^*$  is then hydrogenated *via* intermediate  $\text{CH}_3\text{O}^*$  formation to form methanol.<sup>252,253</sup> A similar r-HCOO mechanism was proposed by Behrens *et al.* The DFT calculation studies revealed that compared to  $\text{PsCu}_3(111)$ , the surface of PdCu (111) with an unsaturated Pd atom is more active for the adsorption and activation of  $\text{CO}_2$  and  $\text{H}_2$ .<sup>253</sup>

#### 4.3 The RWGS + CO-hydro mechanism

In this mechanism,  $\text{CO}_2$  is transformed to CO *via* a  $\text{COOH}^*$  intermediate, then CO is hydrogenated to produce methanol using intermediates HC,  $\text{H}_2\text{CO}$ , and  $\text{H}_3\text{CO}$  and CO is the byproduct.<sup>254–256</sup> While HCO,  $\text{H}_2\text{CO}$ , and  $\text{H}_3\text{CO}$  intermediates directly contribute to the hydrogenation of methanol, CO can still be generated by dissociating  $\text{CO}_2$  without an intermediate. This mechanism has been suggested for Au-based systems such as Au/CeO<sub>x</sub>/TiO<sub>2</sub>.<sup>257</sup>

#### 4.4 The *trans*-COOH mechanism

Hydrocarboxyl  $\text{COOH}^*$  is the first hydrogenated species in this molecular route. COOH is generated when  $\text{CO}_2$  and the H atom of  $\text{H}_2\text{O}$  react.<sup>226,258–260</sup> Methanol is formed when  $\text{COOH}^*$  is further hydrogenated to  $\text{COHOH}^*$ , which is then dissociated to  $\text{COH}^*$  *via* intermediates such as HCOH and  $\text{H}_2\text{COH}$ . This mechanism was proposed over the surface of Au/Cu–ZnO–Al<sub>2</sub>O<sub>3</sub> and Ga<sub>3</sub>Ni<sub>5</sub>.<sup>261,262</sup>

One of the major challenges in methanol synthesis from  $\text{CO}_2$  over heterogeneous catalysts is severe operating conditions including high pressure and temperature. Additionally, the thermodynamics and the continuous separation of methanol

from  $\text{CO}_2$  and byproducts in the recirculating process constrain  $\text{CO}_2$  thermocatalytic hydrogenation. Various methods for  $\text{CO}_2$  reduction to methanol have been developed in recent years, including homogeneous catalysis, photocatalysis, and electrocatalysis. The benefits of the new technologies encompass lower temperatures compared to heterogeneous catalysis, the utilization of alternate energy sources (light or electricity), and the potential for enhanced methanol selectivity.

#### 4.5 Electrocatalytic mechanism

Electrocatalysis is a process in which the catalyst plays a pivotal role by decreasing the activation energy of the reaction *i.e.* accelerating the reaction with faster electron transfer and it remains unchanged at the end. Typically, these electrocatalysts are heterogeneous catalysts as the reactions take place on the surface of the electrocatalyst. The process involves three major steps: (a) reactants adsorb onto the catalyst surface, (b) the chemical reaction takes place on the surface, and (c) the products desorb from the catalyst surface. To evaluate the catalytic activity of different electrode materials, researchers commonly compare the current density at a fixed overpotential or determine the overpotential required to achieve a specific current density. An efficient electrocatalyst demonstrates high current density at low overpotential, indicating both high activity and energy efficiency.<sup>263</sup>

Electrocatalytic processes generally occur in cathodes and anodes of fuel cells and also in electrolysis devices. In the anode, fuel gets oxidized and at the cathode, the oxygen reduction reaction occurs, producing electrical energy. In the anode, various fuels can be used for oxidation purposes, such as methane, ammonia, alcohols, hydrogen and sugars. For the cathode, another alternative can be  $\text{H}_2\text{O}_2$  as an oxidant. A single atom catalyst (SAC) represents the ultimate small size limit of metal particles, which is generally used as a catalyst with the help of a support such as metal oxides, metal surfaces or graphene. The SAC contains isolated atoms singly dispersed on a support. With well-defined dispersion on the support surface, it exhibits maximum efficiency and selectivity. Furthermore, the most efficient way to maximize the utilization of every metal atom in supported metal catalysts is to reduce the metal nanostructures to well-defined, atomically dispersed active centers, known as single-atom catalysts (SACs) (Fig. 7). This represents the ultimate achievement in fine dispersion. For example, Zhang *et al.* developed a practical platinum single-

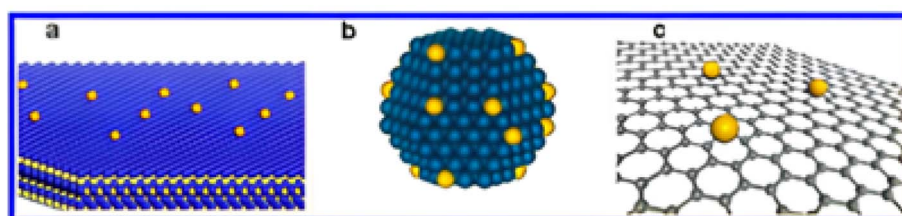


Fig. 7 Schematic diagrams illustrating different types of SACs. Reprinted with permission from ref. 264. Copyright permission from 2013 American Chemical Society.



atom catalyst supported on iron oxide designated as  $\text{Pt}_1/\text{FeO}_x$ .<sup>264</sup> Moreover, the preparation of SACs is very challenging as single atoms tend to get agglomerated. The SACs can be applied in different electrochemical applications, such as the hydrogen evolution reaction (HER), oxygen evolution reaction (OER), oxygen reduction reaction (ORR), nitrogen reduction reaction, and carbon dioxide reaction. The mechanisms of these reactions are discussed in detail in ref. 265.

P. Sharma *et al.* reported a straightforward synthesis strategy for a single-atom ruthenium (Ru) catalyst integrated into a photoactive mesoporous  $\text{C}_3\text{N}_4$  ( $\text{mC}_3\text{N}_4$ ) support. Using the RuSA- $\text{mC}_3\text{N}_4$  catalyst under ambient conditions and visible light, efficient photocatalytic conversion of  $\text{CO}_2$  into methanol was achieved. The process yielded an impressive  $1500 \mu\text{mol g}^{-1}$  of methanol within 6 hours, utilizing a low ruthenium loading of just 0.4 wt%.<sup>266</sup> The image depicts the possible photocatalytic mechanism of the RuSA- $\text{mC}_3\text{N}_4$  catalyst under visible light irradiation during the conversion of  $\text{CO}_2$  to methanol. They have narrowed the band gap compared to other prepared materials which helps to generate more electrons upon visible light irradiation. The incorporated Ru single atom on the  $\text{C}_3\text{N}_4$  network traps electrons from  $\text{C}_3\text{N}_4$  which helps to sustain the photogenerated electron-hole pair for a longer time. As a result, easy electron transfer occurs to reduce  $\text{CO}_2$  which adsorbs on its surface and transforms into methanol (Fig. 8).

Here's an explanation of the process:

#### 1. Photoexcitation (light absorption):

(a) When visible light is irradiated on the catalyst, the electrons present in the valence band of the  $\text{mC}_3\text{N}_4$  photoactive support get excited.

(b) These excited electrons are promoted to the conduction band (CB), leaving behind holes ( $\text{h}^+$ ) in the VB of the same metal.

(c) In this particular case *i.e.* the RuSA- $\text{mC}_3\text{N}_4$  catalyst has a band gap (energy difference between the CB and VB) of approx. 2.50 eV, enabling the absorption of photons from visible light.

#### (2) Electron transfer and catalysis:

(a) After excitation of the electrons to the CB, the electrons are transferred to the Ru single atoms ( $\text{Ru}^{+}$ ) embedded in the  $\text{mC}_3\text{N}_4$  matrix, also reducing the photocarrier transfer barrier. These Ru atoms act as active sites for catalytic reactions.

(b) The electrons reduce  $\text{CO}_2$ , leading to the formation of methanol ( $\text{CH}_3\text{OH}$ ) and side products identified as CO and  $\text{CH}_4$  gases.

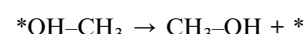
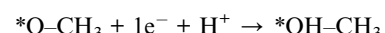
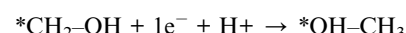
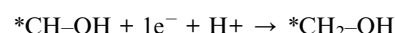
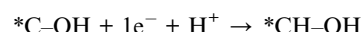
#### 3. Hole utilization:

(a) The holes ( $\text{h}^+$ ) in the VB participate in the oxidation of water ( $\text{H}_2\text{O}$ ), producing oxygen ( $\text{O}_2$ ) and releasing additional protons ( $\text{H}^+$ ).

(b) This step regenerates protons necessary for the reduction process.

#### 4. Reduction and oxidation reactions:

(a) On the CB side, the reduction reactions include: first,  $\text{CO}_2$  gets adsorbed on the surface of the catalyst, reduced to a  $\text{COOH}^*$  intermediate, and then further reduced to CO. Later CO transformed into methanol after 6 steps, as given below:<sup>265</sup>



(b) On the VB side, oxidation reactions occur:



## 5. The catalytic journey of the $\text{CO}_2$ hydrogenation reaction

The review provides a strategic action plan to address the negative impacts of  $\text{CO}_2$  emissions on Earth's ecosystems. The strategy places an emphasis on reducing the use of fossil fuels and implementing catalytic technologies for  $\text{CO}_2$  conversion. Specifically, it focuses on the mixed and electrocatalytic transformation of carbon dioxide to methanol using noble metals. It goes into great detail about thermodynamics, problems, and techniques used in  $\text{CO}_2$  hydrogenation. We present a study of the historical development of catalysts and their industrial

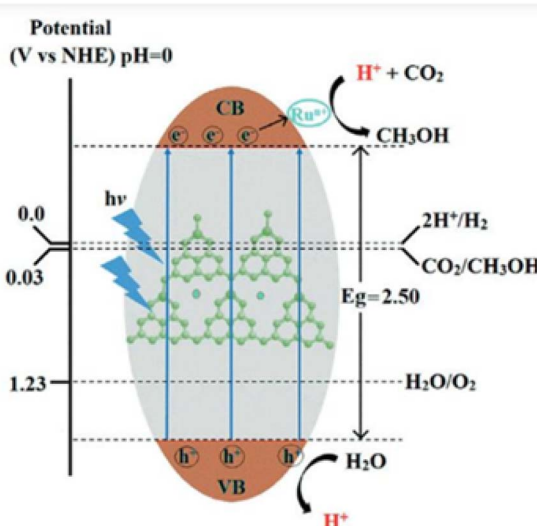


Fig. 8 A plausible schematic illustration of the photocatalysis pathway under visible light irradiation. Reprinted with permission from ref. 266. Copyright permission from 2021 Wiley-VCH GmbH.



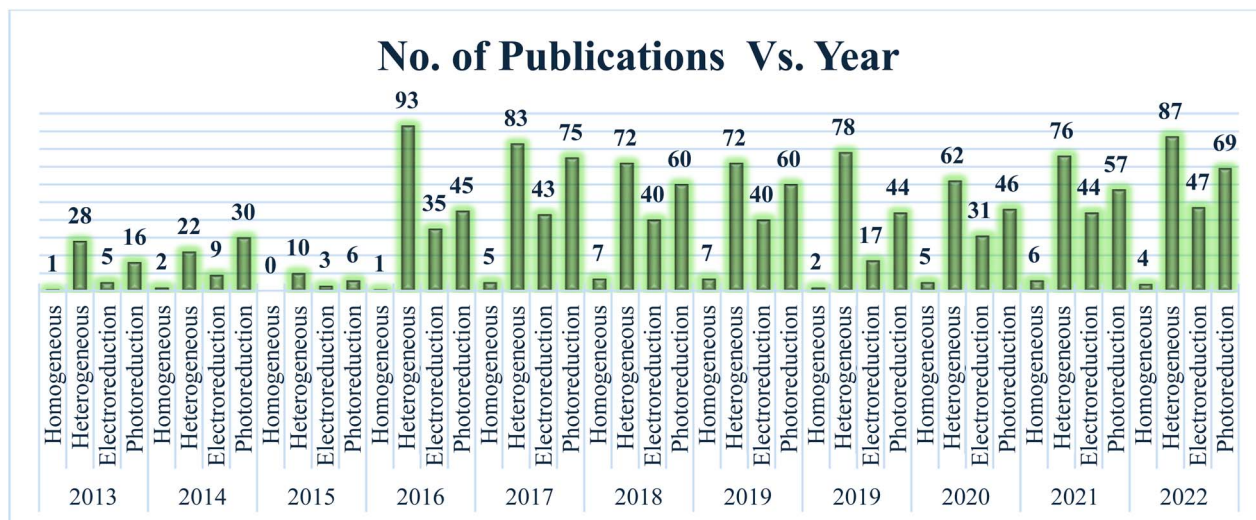


Fig. 9 The number of publications per year during the period of 2013 to 2022.

applications, emphasizing the novel approach towards achieving carbon neutrality. The transformation of carbon dioxide ( $\text{CO}_2$ ) into methanol is a subject of ongoing research and development in the field of catalytic science (Fig. 9). Over time, the discovery of numerous catalysts and the increasing understanding of their behavior and effectiveness have led to significant progress towards a sustainable future. The recognition of the BASF-ZnO- $\text{Cr}_2\text{O}_3$  compound as a catalyst for the reduction of carbon dioxide to methanol in 1920 marked a significant achievement in this area.<sup>267</sup> The discovery of ICI-Cu-ZnO- $\text{Al}_2\text{O}_3$  as an effective catalyst for the same process in 1960 significantly expanded the potential of this conversion.<sup>267</sup> The discovery that Frost made in 1988 on the "Junction Effect Interaction" of catalysts opened up new doors for the creation of catalysts that were more effective.<sup>268</sup> The Nobel Prize for the "Methanol Economy" in 1994 highlighted the importance of converting carbon dioxide into methanol as a means of promoting sustainability. The year 1994 further solidified this concept. Significant progress in the conversion of carbon dioxide to methanol was made possible by the development of catalysts that were supported on nanocrystals of copper in 2002. Subsequently, researchers conducted an investigation into the correlation between oxygen vacancies and reactive flaws in ceria surfaces, leading to the development of even more effective catalysts.<sup>269</sup> The publication of the book "Beyond Oil and Gas: The Methanol Economy" in 2006 heightened awareness of methanol's potential as an environmentally friendly alternative to fossil fuels.<sup>270</sup>

In 2011, the idea of an "Anthropogenic Chemical Carbon Cycle for a Sustainable Future" was presented, with the primary focus being placed on the necessity of converting carbon dioxide into methanol in order to reduce greenhouse gas emissions.<sup>271</sup> The creation of copper-ceria/copper-ceria-titania catalysts in 2014 was a significant step forward, as these catalysts demonstrated increased efficiency in the process of converting carbon dioxide to methanol.<sup>272</sup> In 2017, active sites on

Cu/ZnO catalysts were investigated, yielding significant knowledge on the mechanism of  $\text{CO}_2$  reduction to methanol.<sup>273</sup> The catalyst support primarily scatters the active phase to prevent metal particles from sintering, while also ensuring thermal stability. Numerous experiments have demonstrated that the catalyst support influences the activity and selectivity of the methanol reaction. There are several types of carbon nanofibers (CNFs), including zirconia, silica, alumina, and carbon nanotubes (CNTs).<sup>276-285</sup> In certain instances, a promoter may not yield the desired effect. Furthermore, it has the potential to influence the catalyst's efficiency by either promoting the intended reaction or minimizing the incidence of undesirable reactions. As a result, incorporating promoters has the potential to improve both the product's selectivity and the catalyst's activity. There are several researchers who have documented the utilization of promoters for  $\text{CH}_3\text{OH}$  synthesis catalysts. Some examples of these promoters are gallium oxide ( $\text{Ga}_2\text{O}_3$ ), zinc oxide ( $\text{ZnO}$ ), niobium oxide ( $\text{Nb}_2\text{O}_5$ ), and others.<sup>286-290</sup> The year 2019 saw the discovery of ternary interactions in Cu-ZnO-ZrO<sub>2</sub> catalysts, which extended the possibilities for catalyst development that are even more effective.<sup>291</sup> The year 2020 saw the discovery of the one-of-a-kind interaction that occurs between copper and zinc in the Cu/ZnO system. This discovery opened up new possibilities for the creation of catalysts that are even more efficient.<sup>292</sup> The most recent breakthrough in this area is the creation of a new black indium oxide catalyst in 2022. This catalyst facilitates the effective conversion of carbon dioxide into methanol, which serves as a source of energy and a chemical feedstock, and represents a significant step towards a more sustainable future.<sup>293</sup> The constant process of transforming carbon dioxide into methanol through the application of catalytic technology, defined by countless discoveries and breakthroughs, has been a journey. These achievements are critical milestones in developing a sustainable future and highlight the potential of catalytic science in making the world a better place (Fig. 10).



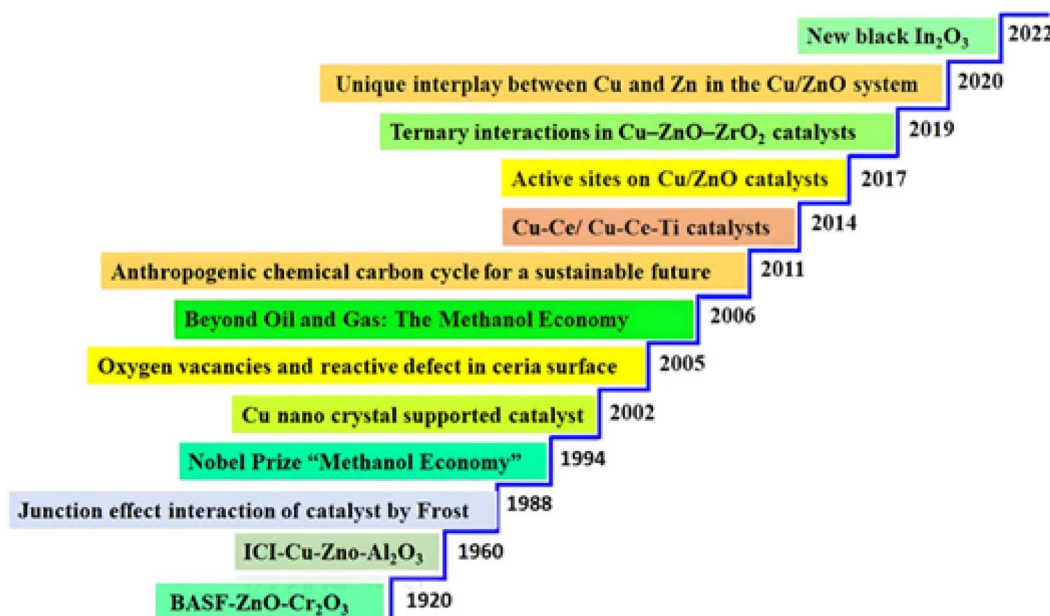


Fig. 10 Some remarkable journeys of hydrogenation of  $\text{CO}_2$  to  $\text{CH}_3\text{OH}$  using heterogeneous catalysts.<sup>83,225,268–273</sup>

### 5.1 Noble metal-based heterogeneous catalysts

In the mid-19th century, heterogeneous catalysts were utilized for the production of  $\text{CH}_3\text{OH}$  from syngas, employing a Cu-ZnO based heterogeneous catalyst in this exothermic process.<sup>294,295</sup> The Cu-ZnO catalyst exhibited significant deactivation and diminished activity with standard syngas, which improved in the late 1990s, followed by the introduction of noble metal-based heterogeneous catalysts that enhanced the hydrogenation conversion of  $\text{CO}_2$  to  $\text{CH}_3\text{OH}$ . Compared with transition metal-based catalysts, noble metal-based catalysts generally have higher activity in the  $\text{CO}_2$  hydrogenation process. For successful  $\text{CO}_2$  hydrogenation, both  $\text{CO}_2$  and  $\text{H}_2$  should be activated simultaneously, and the noble metal nanoparticles are usually more active for  $\text{H}_2$  activation with the enhanced hydrogen spill-over phenomenon than transition metal nanoparticles, hence noble metal-based catalysts usually outperform transition metal-based catalysts in  $\text{CO}_2$  hydrogenation. Furthermore, noble metal nanoparticles are more endurable than transition metal nanoparticles in terms of coke formation, which allows noble metal-based catalysts to have a longer catalytic lifetime. The details about the noble metal-based heterogeneous catalysts for  $\text{CO}_2$  to methanol conversion are discussed as follows.

**5.1.1 Pd based catalysts.**  $\text{CH}_3\text{OH}$  production from  $\text{CO}_2$  is catalyzed using two main catalytic systems: Cu and Pd catalysts, which have good catalytic activity and selectivity.<sup>155,242,296–299</sup> One of the main difficulties in producing methanol from  $\text{CO}_2$  is catalyst deactivation.<sup>300–302</sup> Pd serves as a promoter for the Cu-ZnO catalyst in the hydrogenation of syn-gas to methanol.<sup>303,304</sup> The electronic state of the catalyst affects the interaction between Pd and Cu, with Pd promoting hydrogen spillover and enhancing the stability of the Cu active site against  $\text{CO}_2$  oxidation.<sup>305,306</sup> The alloy phase diagram has shown that Pd-based metal alloy catalysts such as Pd-Zn, Pd-Cu, Pd-Ga, and Pd-In

alloys can be employed for  $\text{CO}_2$  hydrogenation.<sup>307–313</sup> The new active site with high activity is created by changing the chemical properties of the metal surface by employing alloys and ultimately increasing the catalytic activity. The alloy composition depends on the metal composition and reduction conditions to tune the atomic ratio of the two components. Different Pd supported catalysts, including mesoporous MCM-41, SBA-15, and carbon based materials such as CNFs, CNTs, etc., increased catalytic activities and led to the development of various synthetic routes, including CVI (chemical vapour impregnation), citrate decomposition, incipient wetness impregnation, atomic layer deposition etc.<sup>314–317</sup> These methods are crucial for  $\text{CH}_3\text{OH}$  synthesis activity and the development of highly active catalysts at low temperatures.

**5.1.2 Pd-ZnO based catalysts.** The Pd-Zn alloy is one of the notable bimetallic catalysts employed for the synthesis of  $\text{CH}_3\text{OH}$ . In 2004, Iwasa *et al.* reported a Pd/ZnO catalyst for  $\text{CH}_3\text{OH}$  synthesis from  $\text{CO}_2$ .<sup>318</sup> The catalytic performance of Pd/ZnO/ $\text{Al}_2\text{O}_3$  was investigated by Geng and coworkers.<sup>319</sup> Pd-Zn alloys can influence the deactivation of the catalyst for methanol synthesis and stabilize formate intermediates during  $\text{CH}_3\text{OH}$  synthesis, as reported by Bahruji and coworkers. The particle size and oxidation state have a significant impact on the catalytic performance of Pd, as shown by Bahruji and coworkers.<sup>320,321</sup> Liao and co-workers developed the low-pressure methanol synthesis method by utilizing a Zn enriched Pd-Zn core-shell catalyst from sodium selenite, cadmium nitrate, and 5% Pd with ZnO supported (Pd/CdSe-ZnO) precursors. The uniqueness of this catalyst is that it suppresses the CO production by the RWGS reaction.<sup>322</sup> Zaman and co-workers were the first to report Ca doped Pd-Zn on the  $\text{CeO}_2$  catalyst for methanol synthesis from  $\text{CO}_2$  hydrogenation. It was observed that  $\text{CeO}_2$ -supported PdZn showed high

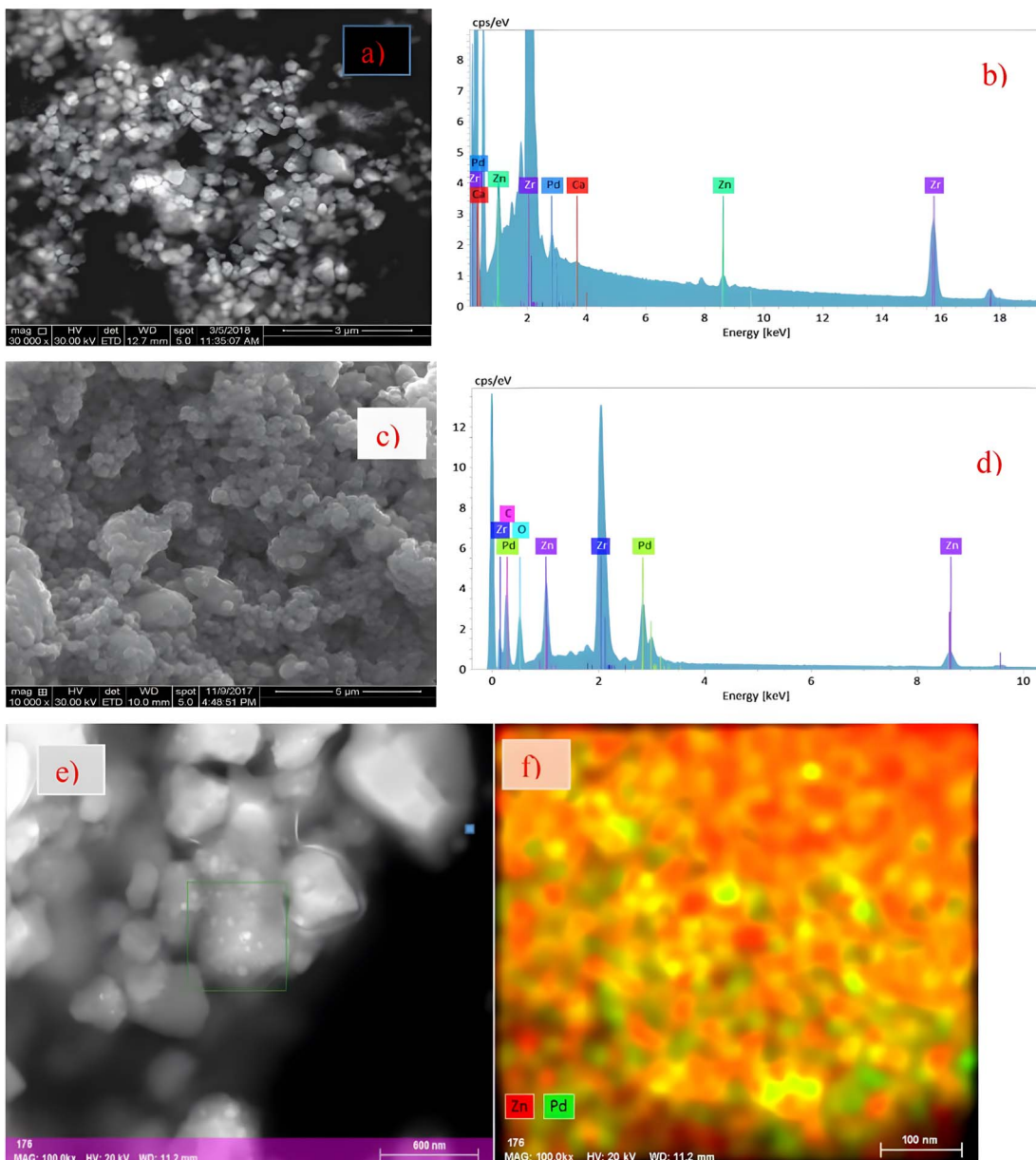


Fig. 11 Electron microscopy and spectroscopy of spent catalyst 0.5Ca5P5Zr-IMP. SEM image (a) and corresponding energy dispersive spectrum (EDS) (b) of 0.5Ca5P5Zr-IMP, SEM image (c) and EDS (d) of 5P5Zr-IMP. Surface mapping (e) and Pd/Zn distribution (f) in 5P5Zr-IMP.<sup>323</sup> Copyright 2019 Elsevier.

selectivity in catalytic activity and Ca-doped PdZn/CeO<sub>2</sub> showed 100% methanol selectivity at low temperatures<sup>323</sup> (Fig. 11). Diez-Ramirez and coworkers reported a carbon nanofiber-based PdZn catalyst for methanol synthesis from CO<sub>2</sub> at atmospheric pressure, with the performance of the catalyst dependent on the particle size.<sup>324</sup> In recent years, Yerga *et al.* synthesized PdZn-ZnO catalysts on TiO<sub>2</sub> with Zn/Pd molar ratios of 2.5, 5, and 7.5 using metal organic precursors. The experimental studies reveal that the catalyst with the highest ZnO content achieved the best methanol yield (78.9 mmol<sub>MeOH</sub> min<sup>-1</sup> mol<sub>Pd</sub><sup>-1</sup>) due to enhanced CO<sub>2</sub> adsorption, greater ZnO particle stability, and intermediate hydrogenation.<sup>325</sup> Tian and coworkers synthesized a Pd/ZnO single atom

catalyst for methanol steam reforming. The experimental studies showed that the TOF of 2PdZn/Al<sub>2</sub>O<sub>3</sub> NP is 1.4 times that of 0.2PdZn SAC.<sup>326</sup>

**5.1.3 Pd-Cu based catalysts.** There has been a surge in research utilizing bimetallic Pd-Cu catalysts for the synthesis of methanol from CO<sub>2</sub>. Jiang *et al.* examined the utilization of SiO<sub>2</sub>-supported Pd-Cu catalysts in the process and determined that the partial pressure has a significant impact on CO<sub>2</sub> hydrogenation. The use of bimetallic catalysts was found to enhance the activity and reduce the selectivity of methanol. A kinetic study showed that the synthesis of CH<sub>3</sub>OH was dependent on the H<sub>2</sub>/CO<sub>2</sub> ratio and that the Pd-Cu bimetallic catalyst played an active role.<sup>327</sup>

This group reported another study that elaborated on the connection between the size effect, surface alloy composition and catalytic efficiency. This work mainly focused on the manufacture of a Pd–Cu bimetallic catalyst; the ratio of Pd/(Pd + Cu) lies within 0.25–0.34 and is used for the hydrogenation of CO<sub>2</sub> to produce CH<sub>3</sub>OH. The main observation is that Pd–Cu(2.4)/SiO<sub>2</sub>, which has a lower metal loading than a commercial catalyst, produces 2 times as much CH<sub>3</sub>OH at 523 K and 4.1 MPa concerning metal-based space-time yield (STY).<sup>328</sup> Lin *et al.* conducted an investigation into the use of various supports, including TiO<sub>2</sub>, ZrO<sub>3</sub>, CeO<sub>3</sub>, Al<sub>2</sub>O<sub>3</sub>, and SiO<sub>2</sub>, for the Pd–Cu catalyst. The results indicated that TiO<sub>2</sub> and ZrO<sub>2</sub> showed the highest activity for methanol synthesis. The adsorption capacity for methanol synthesis is attributed to the influence of metal support interaction on the process, with the Pd–Cu catalysts facilitating the bonding between H<sub>2</sub> and CO<sub>2</sub> on the surface.<sup>329</sup> The changes in metal–support interactions were primarily attributed to enhancing moderate interactions between the metal and support, which aimed to boost adsorption capacity and promote methanol synthesis. This study supported the idea that Pd–Cu catalysts play a significant role in shifting adsorption toward bonding between H<sub>2</sub> and CO<sub>2</sub> on the alloy surface.

**5.1.4 Pd–Ga catalysts.** Several research studies have been conducted to explore the use of Pd–Ga<sub>2</sub>O<sub>3</sub> catalysts for methanol synthesis from CO<sub>2</sub>. Fujitani *et al.* reported that the Pd–Ga<sub>2</sub>O<sub>3</sub> catalyst showed higher catalytic activity compared to the commonly used Cu/ZnO catalyst.<sup>330</sup> In 2002 Collins *et al.* reported that dissociated atomic hydrogen spillover from metallic Pd to Ga<sub>2</sub>O<sub>3</sub> causes Pd NPs to accelerate the hydrogenation rate of carbonaceous species chemisorbed over the surface of b-Ga<sub>2</sub>O<sub>3</sub>.<sup>331</sup> Behrens *et al.* synthesized a series of Pd–Ga catalysts consisting of intermetallic compounds, and found that gamma Ga<sub>2</sub>O<sub>3</sub> played a significant role in the selective hydrogenation of

methanol.<sup>332</sup> Damsgaard and co-workers synthesized a non-dispersed intermetallic GaPd<sub>2</sub>/SiO<sub>2</sub> catalyst for the synthesis of methanol from CO<sub>2</sub>. This intermetallic catalyst showed higher catalytic activity than Cu/Zn/Al<sub>2</sub>O<sub>3</sub> which was the most used catalyst. *Ex situ* and *in situ* characterization techniques, reveal that different aspects of the catalytic structure show a good correlation between the results at various pressures. The TEM study introduced a deeper evaluation of the dynamic catalytic activity during methanol synthesis at atmospheric pressure.<sup>333</sup> Tsang and co-workers reported that the interaction of Pd and Ga<sub>2</sub>O<sub>3</sub> nanocrystals with a predominant 002 surface on metal supports resulted in enhanced catalytic activity for the synthesis of methanol from CO<sub>2</sub> hydrogenation. This work emphasizes electron transfer from Ga<sub>2</sub>O<sub>3</sub> to Pd NPs (nano particles) thereby enhancing the reduction process of Ga<sup>3+</sup> and directly enriching the conversion process from CO<sub>2</sub> to methanol.<sup>334</sup> Williams and co-workers synthesized a colloidal Pd<sub>2</sub>Ga-based catalyst by thermal decomposition of Pd(II) acetate in the presence of the Ga(III) state. Various characterization techniques, such as HR-TEM, STEM, XPS, and XRD support the formation of Pd<sub>2</sub>Ga nanoparticles with an average diameter of 5–6 nm. This work is considered the benchmark of methanol synthesis and the Pd/Ga colloidal catalyst shows promising stability and higher catalytic activity than the Cu–ZnO–Al<sub>2</sub>O<sub>3</sub> catalyst for the conversion of CO<sub>2</sub> to methanol.<sup>335</sup> Michael Bowker and his colleagues conducted another intriguing study. This study examines the Pd deposition on Ga<sub>2</sub>O<sub>3</sub> and In<sub>2</sub>O<sub>3</sub> for CO<sub>2</sub> hydrogenation to methanol. The interesting finding in this work is that Ga<sub>2</sub>O<sub>3</sub> is active alone, but In<sub>2</sub>O<sub>3</sub> achieves high conversion and 89% methanol selectivity.<sup>336</sup>

Morgan and coworkers<sup>336</sup> synthesized a nanodispersed intermetallic GaPd<sub>2</sub>/SiO<sub>2</sub> catalyst; industrially relevant high-surface-area SiO<sub>2</sub> is impregnated with Pd and Ga nitrates, then dried, calcined, and reduced in hydrogen (Fig. 12). The

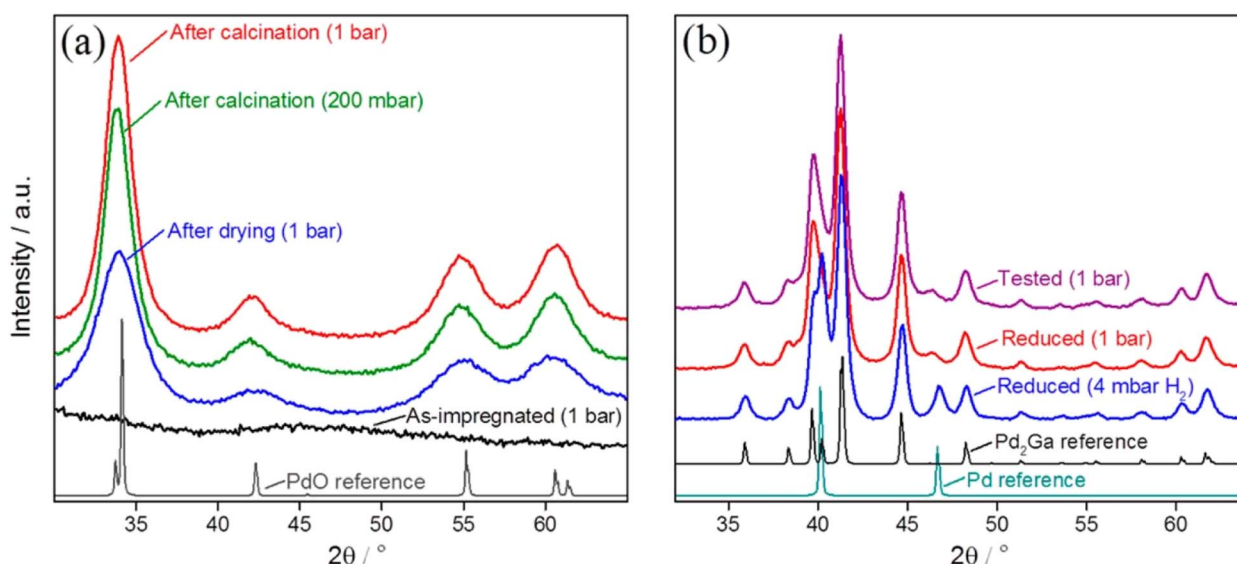


Fig. 12 (a) XRD patterns obtained from the impregnated, dried, and calcined catalyst precursor at room temperature and atmospheric pressure, and (b) from the reduced and tested GaPd<sub>2</sub>/SiO<sub>2</sub> catalyst for CO<sub>2</sub> hydrogenation. Reprinted with permission from ref. 333. Copyright 2015 American Chemical Society.



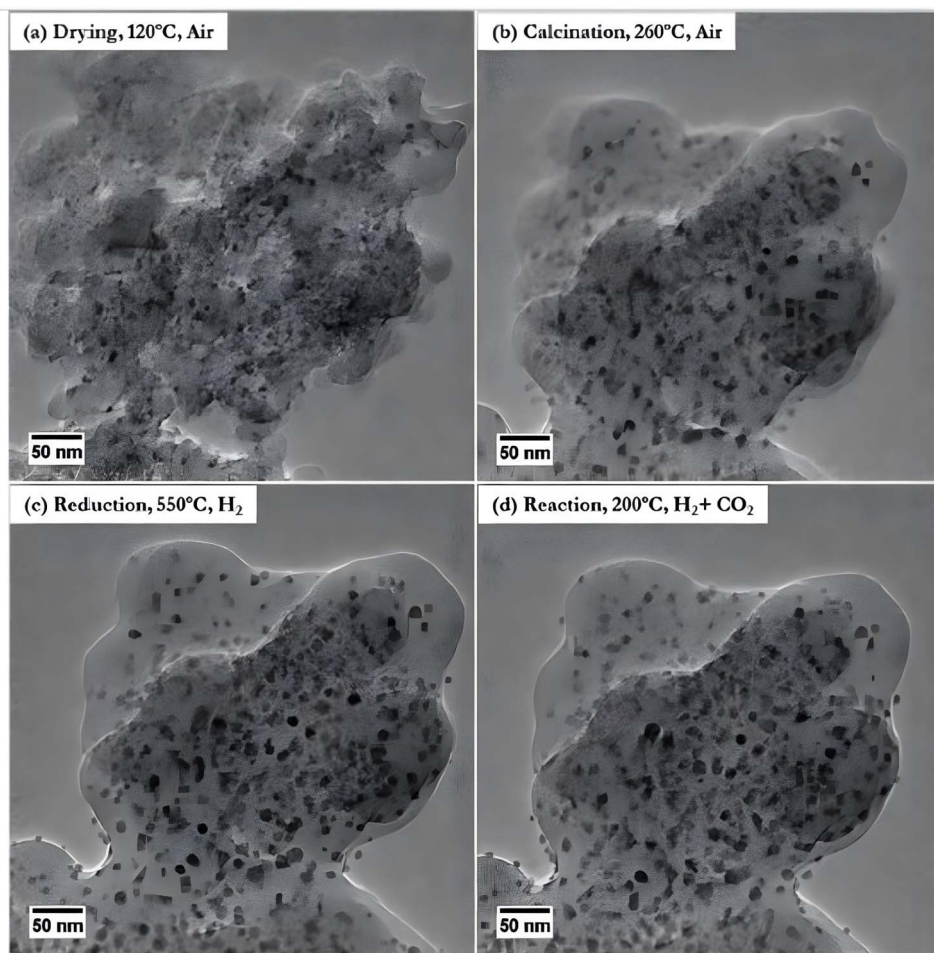


Fig. 13 IL-TEM images of the  $\text{GaPd}_2/\text{SiO}_2$  catalyst acquired after drying (a), calcination (b), reduction (c), and methanol synthesis (d).<sup>333</sup> Copyright 2015 American Chemical Society.

$\text{GaPd}_2/\text{SiO}_2$  catalyst outperforms the traditional  $\text{Cu}/\text{ZnO}/\text{Al}_2\text{O}_3$  catalyst for  $\text{CO}_2$  hydrogenation to methanol at ambient pressure. Additionally, it produces less unwanted CO. The  $\text{GaPd}_2/\text{SiO}_2$  catalyst is investigated using both *in situ* and *ex situ* approaches (Fig. 13).

**5.1.5 Pd-In based catalysts.** Pd-In-based catalysts have emerged as a promising option for the production of methanol from  $\text{CO}_2$  due to the presence of oxygen vacancies, which allow for the adsorption of carbon dioxide. The catalytic activity of these catalysts can be improved through catalytic activation. García-Trento *et al.* proposed a bimetallic PdIn nanoparticle synthesized by the thermal decomposition of  $\text{Pd}(\text{acetate})_2$  and  $\text{In}(\text{acac})_3$ . This Pd/In (5–10 nm) nanoparticle catalyst showed improved > 80% methanol selectivity at 270 °C compared to the reference  $\text{Cu}/\text{ZnO}/\text{Al}_2\text{O}_3$  catalyst.<sup>337</sup> Snider *et al.* synthesized Pd-In-based catalysts with different In/Pd ratios (1 : 0, 2 : 1, 1 : 1, 1 : 2, and 0 : 1) and enhanced the methanol synthesis process from  $\text{CO}_2/\text{H}_2$  at 40 bar and 300 °C. The highest methanol selectivity of 61% was achieved using the In : Pd (2 : 1)/ $\text{SiO}_2$  catalyst. *In situ* XAS characterization technique revealed that the synergistic effect of the intermetallic compound indium–palladium enhances the selectivity and activity of methanol synthesis.<sup>338</sup>

Liu *et al.* synthesized Pd/ $\text{In}_2\text{O}_3$  catalysts by thermal treatment of  $\text{In}_2\text{O}_3$  powder with a Pd/peptide composite. The Pd/ $\text{In}_2\text{O}_3$  catalyst showed higher activity of methanol synthesis from  $\text{CO}_2$  conversion *i.e.* >20% and methanol selectivity of 70%.<sup>339</sup> Jeschke and coworkers developed the catalyst Pd– $\text{In}_2\text{O}_3$ – $\text{ZrO}_2$  by flame spray pyrolysis methods for the conversion of  $\text{CO}_2$  to methanol. Its high and persistent methanol productivity can be explained by the improved formation of oxygen vacancies revealed by this particular catalyst architecture, according to a ground-breaking procedure designed to quantify them using *in situ* electron paramagnetic resonance spectroscopy.<sup>340</sup> Recently, Cai *et al.* have reported that hollow  $\text{In}_2\text{O}_3$  supported Pd based catalysts are suitable for  $\text{CO}_2$  hydrogenation to methanol. The main finding of this work is that the hollow morphology of  $\text{In}_2\text{O}_3$  supported Pd based catalysts led to higher catalytic performance (10.5%  $\text{CO}_2$  conversion, a methanol selectivity of 72.4% and a methanol space time of 0.53  $\text{g}_{\text{MeOH}} \text{h}^{-1} \text{g}_{\text{cat}}^{-1}$  over 100 h on stream at 3 MPa and 295 °C) compared to  $\text{In}_2\text{O}_3$  nanotube or nanorod morphology.<sup>341</sup> Jiang and coworkers reported the use of an  $\text{In}_2\text{O}_3$ /SBA-15-supported Pd-based catalyst and observed a  $\text{CO}_2$  conversion rate of 12.6% with 83.9% methanol selectivity.<sup>342</sup> Hua and coworkers developed the Pd/ $\text{In}_2\text{O}_3$

nanocatalyst by employing innovative electrostatic self-assembly methods. This catalyst exhibited an increase in the concentration of oxygen vacancies which enhanced the methanol production. This catalyst led to a space time yield (STY) of  $0.54 \text{ g}_{\text{MeOH}} \text{ h}^{-1} \text{ g}_{\text{cat}}^{-1}$  ( $300^\circ\text{C}$ ,  $3.5 \text{ MPa}$ ,  $21\,000 \text{ mL g}_{\text{cat}}^{-1} \text{ h}^{-1}$ ).<sup>343</sup>

**5.1.6 Mesoporous molecular sieves supported Pd-based catalysts.** Song and co-workers reported a nanostructured Pd-based catalyst by the incorporation of mesoporous MCM-41 and SBA-15 and created a nano-sized pore channel using alkali/alkaline earth metal additives, where they observed the addition of an alkali/alkaline earth metal as a promoter enhanced the catalytic activity of methanol synthesis from  $\text{CO}_2$ .<sup>344-346</sup>

The CNT-supported Pd-based catalyst shows high catalytic activity for methanol synthesis. Zhang and coworkers synthesized Pd-ZnO supported multi-walled carbon nanotube-based catalysts showing a high rate of catalytic conversion of methanol from  $\text{CO}_2$ . A large amount of hydrogen is reversibly adsorbed using CNT-supported Pd-ZnO catalysts, which boosts the concentration of active H-species at the surface of the working catalyst and accelerates the kinetics of the hydrogenation reaction.<sup>347</sup> Kong and co-workers developed a MWCNT supported Pd-Ga catalyst for the synthesis of methanol by hydrogenation. This catalyst improved the molar percentage of catalytic activity of  $\text{Pd}^0$  species and also increased the catalytic activity of adsorbing/activating  $\text{H}_2$ .<sup>348</sup> Li *et al.* investigated the Pd nanoparticle supported inside and outside CNT-based catalysts. Higher catalytic activity and methanol selectivity are displayed inside the Pd/CNTs than outside. The turnover frequency of Pd/CNTs (inside) is 3.7 times higher than that of outside-supported CNTs. The selectivity difference between inside and outside CNT-based catalysts is due to the relative concentration of Pd<sup>+</sup> species.<sup>349</sup>

Pd metal actively influences the chemical and electronic properties of the catalyst surface. Furthermore, it is impossible to overstate the importance of Pd's role in converting  $\text{H}_2$  into H-add species and permitting them to overflow onto support surfaces because this is still an essential step in the synthesis of methanol, without which hydrogenation cannot proceed properly. The Pd precursor employed for the synthesis of the catalyst will also affect its overall performance.

**5.1.7 Effect of Pd as a promoter.** In chemistry, catalyst promoters play an important role by improving the catalytic activity and selectivity. In this section, we have discussed the role of Pd as a promoter and its direct influence on the physicochemical properties of the  $\text{CO}_2$  hydrogenation reaction and enhancing the surface area and mechanical strength of the catalyst.

The promoters on a Pd surface enhance the  $\text{CO}_2$  adsorption capacity by generating an electrostatic field. Cabrera *et al.* observed that Pd itself acts as a promoter which increases the catalytic activity of  $\text{Cu} + \text{ZnO}$  ( $\text{Al}_2\text{O}_3$ ) and improves the rate of hydrogenation of  $\text{CO}_2$  due to the hydrogen dissociated on the surface of Pd particles and spillover on the surface of the  $\text{Cu} + \text{ZnO}$  catalyst. In another remarkable study established by Lee and co-workers, the catalytic activity of  $\text{Cu}/\text{CeO}_2$  was increased by the addition of a small amount of Pd. A small amount of Pd is

added to the  $\text{Cu}/\text{CeO}_2$  catalyst to facilitate the reactivity of Cu sites, which in turn increases methanol productivity. The interaction with highly dispersed Pd increases the surface and dispersion concentration of Cu. The transfer of electrons from palladium to copper leads to a reduction in copper sites, while the addition of palladium as a promoter diminishes the surface area of cerium dioxide. So, it can be concluded that the rate of hydrogenation of  $\text{CO}_2$  and methanol productivity can be increased with the addition of a small amount of Pd to the  $\text{Ce}/\text{CeO}_2$  catalyst.<sup>350</sup> Hu *et al.* reported Pd promoted Cu-ZnO catalysts for the synthesis of a series of Pd doped Cu-ZnO catalysts with a constant Cu/Zn ratio (1:1) and varied Pd molar ratios from 0.01 to 0.04 mol%. It was observed that the 1% Pd doped Cu-ZnO catalyst promotes the methanol space-time yield by 2.5 times and turnover frequency (TOF) by 3.5 times at  $543^\circ\text{K}$  as compared to the undoped Cu-ZnO catalyst. Tsang *et al.* investigated the effect of the promoter Pd on the  $\text{Pd}/\text{ZnO}/\text{Al}_2\text{O}_3$  catalyst. The result indicated that methanol selectivity depends on the ratio of  $\text{Pd}^0/\text{PdZn}$  and the EXAFS study showed that the Pd-modified ZnO<sub>x</sub> possesses an active site for methanol synthesis.<sup>305</sup> Koizumi *et al.* investigated the incorporation of Pd nanoparticles into mesoporous supports such as MCM-41, and SBA-15 with promotion using alkali/alkaline earth metals synthesized by incipient wetness impregnation. It was observed that without impregnation of any promoters, Pd-supported mesoporous silica showed weak activities towards methanol synthesis, but the addition of alkali or alkaline earth metals such as K, Mg, and Ca increased the catalytic activities of K(Ca) promoted Pd-supported mesoporous SBA-15 producing two times higher methanol yield than that of Pd-supported mesoporous silica. Song and co-workers synthesized Pd supported catalysts by the impregnation method with  $\text{Pd}(\text{NO}_3)_2$ . CaO promoted the  $\text{CO}_2$  hydrogenation activity with the highest selectivity for methanol over Pd/MCM-41.<sup>344</sup> Yin and co-workers reported a metal-organic framework-based PdZnO catalyst from the Pd@zeolitic imidazolate framework (ZIF-8) for hydrogenation of  $\text{CO}_2$ . The formation of small-sized PdZn alloy particles after  $\text{H}_2$  reduction and the abundance of surface oxygen defects on ZnO are crucial for such a high methanol production. The SMSI between PdZn and ZnO also ensures the long-term stability of the PdZn catalysts. Lastly, it can be proposed that the active site strongly associated with methanol formation is the PdZn alloy rather than metallic Pd.<sup>351</sup>

#### (i) Au based catalysts

Researchers have discovered that gold nanoparticles act as highly active catalysts for  $\text{CO}_2$  hydrogenation. Vourros *et al.* successfully investigated the activity of Au nanoparticles supported on various oxides ( $\text{M}_x\text{O}_y - \text{Al}_2\text{O}_3$ ,  $\text{TiO}_2$ ,  $\text{Fe}_2\text{O}_3$ ,  $\text{CeO}_2$ , and  $\text{ZnO}$ ) to catalyze the synthesis of methanol from the hydrogenation of  $\text{CO}_2$ . Au nanoparticles based on  $\text{Au}/\text{CeO}_2$  (82%) and  $\text{Au}/\text{ZnO}$  (90%) show high selectivity towards  $\text{CH}_3\text{OH}$  synthesis at temperature below  $250^\circ\text{C}$ .<sup>352</sup> Behm and co-workers synthesized metal oxide-supported Au catalysts ( $\text{Au}/\text{Al}_2\text{O}_3$ ,  $\text{Au}/\text{TiO}_2/\text{Au}/\text{ZnO}$ , and  $\text{Au}/\text{ZrO}_2$ ) for the synthesis of 'green methanol' from  $\text{CO}_2$ . The Au/ZnO catalyst is one of the potential candidates for green methanol technology. With an increase in the diameter of Au nanoparticles in the Au/ZnO catalyst, the rate of methanol



Table 1 The summary of noble-metal based catalysts for the hydrogenation of CO<sub>2</sub> to methanol

| Catalyst   | CO <sub>2</sub> /H <sub>2</sub> ratio | Temp./K | MPa | Space velocity | Conv. | Selectivity | STY       | Ref. |
|--|---------------------------------------|---------|-----|----------------|-------|-------------|-----------|------|
| Pd/ZnO   | 1:3                                   | 523 K   | 2   | 3600(W)        | 10.7  | 60          | 77.4      | 320  |
| PdZn-400   | 1:3                                   | 543 K   | 4.5 | 21 600(W)      | 15.1  | 56.2        | 650       | 365  |
| Pd/Ga <sub>2</sub> O <sub>3</sub>                    | 1:3                                   | 523 K   | 5   | —              | 19.6  | 51.5        | c.a 20.8  | 334  |
| Pd-In <sub>2</sub> O <sub>3</sub> (Co-precipitation) | 1:4                                   | 553 K   | 5   | 24 000         | —     | 75          | 0.061     | 366  |
| Pd(0.25-Cu/SiO <sub>2</sub>                          | 1:3                                   | 250 °C  | 41  | 3600           | 6.7   | 30          | 0.03      | 367  |
| Pd/SiO <sub>2</sub>                                  | 1:3                                   | 523 K   | 2   | —              | 0.33  | 31.6        | 0.013     | 349  |
| Pd/Cu-P25  | 1:3                                   | 523 K   | 4.1 | —              | 16.4  | 25.7        | 1.80      | 368  |
| Pd/In <sub>2</sub> O <sub>3</sub>                    | 1:4                                   | 300 °C  | 50  | 21 000         | 20    | 72          | 0.89      | 369  |
| Pd-Pt/In <sub>2</sub> O <sub>3</sub>                 | 1:4                                   | 300 °C  | 5   | 21 000         | 17.7  | 68.3        | 0.725     | 370  |
| PdZn/ZnO-3.93Al                                      | 1:3                                   | 523 K   | 3.0 | —              | 14.2  | 51.6        | c.a 4.51  | 371  |
| Pd/Zn SiO <sub>2</sub>                               | 1:3                                   | 260 °C  | 3   | —              | 2.6   | 11.2        | 0.03      | 372  |
| 2Pd/CeO <sub>2</sub> -R                              | 1:3                                   | 240     | 3   | 2000           | 6.2   | 29          | 0.012     | 373  |
| 5% Pd/ZnO, IM  | 1:3                                   | 523 K   | 2.0 | —              | 8.7   | 1           | 0.055     | 320  |
| 0.5Ca <sub>5</sub> Pd <sub>5</sub> ZnZr              | 1:3                                   | 523 K   | 3.0 | 2400           | 14.2  | 51.6        | c.a 4.51  | 374  |
| Pd-Cu/SBA-15   | 1:3                                   | 250 °C  | 4.1 | 3600(W)        | 6.5   | 23          | 23        | 375  |
| Pd/Zn/CNTs   | 1:3                                   | 250 °C  | 3   | 1800(W)        | 6.3   | 99.6        | 37.1      | 376  |
| Pd Cu/CeO <sub>2</sub>                               | 1:3                                   | 523 K   | 4.1 | —              | 9.9   | 28.4        | 1.37      | 368  |
| Pd/TiO <sub>2</sub>                                  | 1:3                                   | 523 K   | 5   | —              | 15.5  | 3.9         | c.a. 1.21 | 377  |
| Pd-P/In <sub>2</sub> O <sub>3</sub>                  | 1:4                                   | 498 K   | 5   | —              | Ca 3  | Ca 95       | 6.01      | 339  |
| Pd/In <sub>2</sub> O <sub>3</sub> /SBA-15            | 1:4                                   | 533 K   | 5   | —              | 12.6  | 83.9        | 11        | 314  |
| Pd-ZnZrO <sub>x</sub>                                | 1:4                                   | 320 °C  | 5   | 24 000         | 16    | 58          | 0.63      | 378  |
| Pt/In <sub>2</sub> O <sub>3</sub>                    | 1:4                                   | 300 °C  | 5   | 21 000         | 17.6  | 54          | 0.542     | 379  |
| Pt/In <sub>2</sub> O <sub>3</sub>                    | 1:3                                   | 300 °C  | 4   | 24 000         | 8.8   | 71.5        | 0.480     | 380  |
| Rh/In <sub>2</sub> O <sub>3</sub> -ZrO <sub>2</sub>  | 1:4                                   | 300     | 5   | 21 000         | 18.1  | 66.5        | 0.684     | 381  |
| UiO-67-Pt  | —                                     | 170     | 0.8 | 6000           | 1.5   | 19.0        | 0.0024    | 382  |
| Au/ZnO   | 1:3                                   | 240 °C  | 0.5 | 4800(G)        | 0.3   | 82          | N/A       | 383  |
| Ag/ZrO <sub>2</sub>                                  | 1:3                                   | 240     | 80  | 3600           | —     | 55          | 359       |      |
| Ag/In <sub>2</sub> O <sub>3</sub>                    | 1:4                                   | 300 °C  | 5   | 21 000         | 13.6  | 58.2        | 0.450     | 384  |
| Au/In <sub>2</sub> O <sub>3</sub> -ZrO <sub>2</sub>  | 1:3                                   | 250     | 50  | 21 000(G)      | 5.0   | 90          | 0.59      | 385  |
| Au/Al <sub>2</sub> O <sub>3</sub>                    | 1:3                                   | 220     | 5   | 24 000(W)      | 2.0   | 3.8         | 383       |      |
| Au/CeO <sub>2</sub>                                  | 1:3                                   | 240     | 5   | 9000           | 1-2   | 40          | 0.412     | 386  |
| Au/In <sub>2</sub> O <sub>3</sub>                    | 1:4                                   | 300     | 5   | 21 000         | 11.7  | 67.8        | 0.47      | 387  |

formation reduces and the selectivity of methanol increases from 56% to approximately 82%.<sup>353</sup> This group also reported better catalytic behaviour of the Au/ZnO-based catalyst for the synthesis of methanol than the conventional Cu-Zn-Al catalyst. From the kinetic and IR spectrophotometer studies, it is revealed that the conversion of CO<sub>2</sub> to methanol proceeds through the formation of formate and methoxy intermediates initiated using the proposed Au/ZnO catalyst.<sup>354</sup> Han *et al.* reported an Au-supported ZrO<sub>2</sub> catalyst for methanol synthesis with a selectivity rate of 73% at 180 °C.<sup>355</sup> The electrical polarization at the metal oxide CeO<sub>x</sub>/TiO<sub>2</sub> anchored with Au nanoparticle-based substrates, as proposed by Chen *et al.*, actively promoted CO<sub>2</sub> adsorption under low pressure conditions and led to greater selectivity of methanol production. According to the AP-XPS study, Au possesses a partial negative charge and CeO<sub>x</sub> shows a Ce<sup>3+</sup> state. The DFT calculation studies supported the substantial charge redistribution occurring at Au<sub>3</sub>/CeO<sub>x</sub>/TiO<sub>2</sub>(110), with Au atoms becoming negatively charged, and negatively charged Au and the positively charged Ce<sup>3+</sup> site bind to the positively charged C atom and the negatively charged O atom of CO<sub>2</sub>, respectively.<sup>356</sup> Rodriguez and coworkers investigated the catalytic properties of In/Au(111) alloys and InO<sub>x</sub>/Au(111) inverse systems for CO<sub>2</sub> hydrogenation by employing AP-XPS studies and batch reactors. The experimental evidence shows that InO<sub>x</sub>/Au(111) demonstrates

significant potential for CO<sub>2</sub> hydrogenation combining high activity and selectivity for methanol production.<sup>357</sup>

#### (ii) Ag-based catalysts

Ag-based catalysts received less attention than Pd and Au-supported catalysts for the hydrogenation of CO<sub>2</sub>.<sup>358</sup> Grabowski *et al.* investigated the catalytic activity of Ag/ZrO<sub>2</sub> and Ag/ZrO<sub>2</sub>/ZnO catalysts. The XPS and Auger spectroscopic techniques confirmed the electronic state of silver and the contents of the zirconia polymorphic phases (tetragonal and monoclinic). The presence of oxygen vacancies in ZrO<sub>2</sub> directly influenced the thermodynamically unstable t-ZrO<sub>2</sub> and Ag<sup>+</sup> species connected with oxygen vacancies thereby accelerating the active phase for methanol synthesis.<sup>359</sup>

#### (iii) Pt/Rh based catalysts

In heterogeneous reactions, dispersed catalysts have a remarkable place due to the low coordination environment of the metal center, quantum size, and SMSI effect.<sup>360</sup> Zheng *et al.* prepared atomically dispersed Pt/MoS<sub>2</sub> catalysts with Pt amounts up to 7.5% and reported that the synergistic interaction between neighboring Pt monomers reduces the activation energy and enhances the catalytic activity relative to isolated Pt monomers in CO<sub>2</sub> hydrogenation. Unlike isolated Pt monomers, neighboring Pt monomers hydrogenate CO<sub>2</sub> sequentially into formic acid and methanol.<sup>361</sup> Song *et al.* investigated a PtCo alloy-based catalyst for methanol synthesis where zigzag Pt-Co



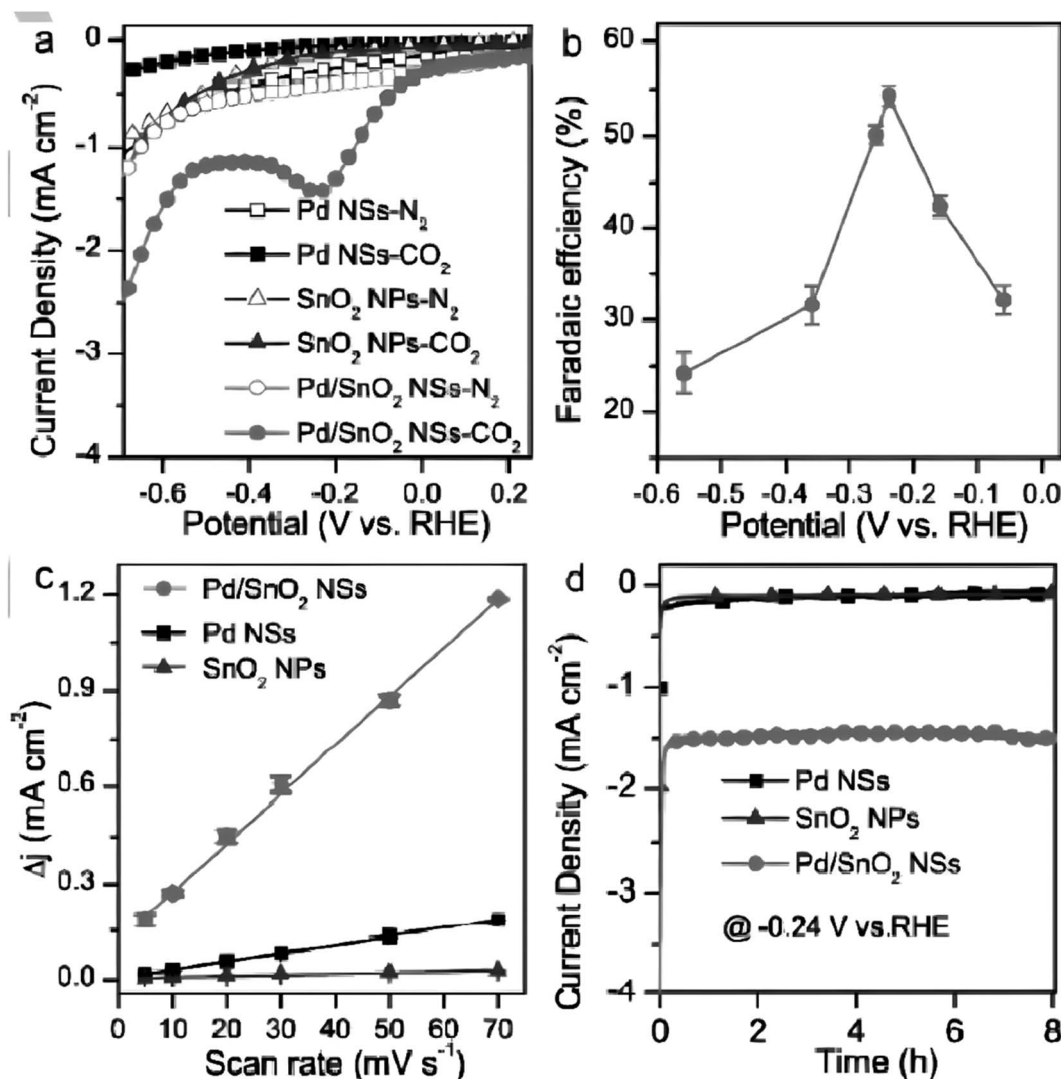


Fig. 14 Electrochemical characterization studies of  $\text{Pd/SnO}_2$  NSs ( $\text{Pd} : \text{Sn} = 1 : 1$ ) in comparison with  $\text{Pd}$  NSs and  $\text{SnO}_2$  NPs. (a) LSV curves obtained in  $0.1 \text{ M NaHCO}_3$  solution. (b) FE for  $\text{CH}_3\text{OH}$  at various applied potentials. (c) Charging current density differences plotted against scan rates. (d) Chronoamperometry studies of different catalysts. Reprinted with permission from ref. 390. Copyright permission from 2018 Wiley-VCH Verlag GmbH & Co. KGaA, Weinheim.

nanowires with a Pt-rich surface and abundant step/edges (defects) were utilized to obtain high catalytic activity.  $\text{Pt}_4\text{Co}$  NWs/C showed the best performance among other PtCo alloys.<sup>303</sup> Analysis using Fourier transform infrared spectroscopy demonstrated that when  $\text{Pt}_4\text{Co}$  NWs/C was used as a catalyst, the process involved  $\text{CO}_2$  adsorption and activation *via* a carboxylate intermediate, resulting in enhanced  $\text{CH}_3\text{OH}$  yield. Shimizu *et al.* investigated a Pt nanoparticle loaded  $\text{MoO}_x/\text{TiO}_2$  catalyst for the hydrogenation of  $\text{CO}_2$  to produce  $\text{CH}_3\text{OH}$  in 73% yield under mild conditions. The X-ray absorption fine structure study suggested that reducing the  $\text{MoO}_x$  species promoted the hydrogenation reaction.<sup>362</sup> Han *et al.* investigated that the methanol selectivity of  $\text{In}_2\text{O}_3$  increased (72.2% to 91.1%) by introducing a small amount of Pt.<sup>363</sup> Zeng and co-workers reported that the RhW alloy with a nanosheet structure acts as a catalyst for the synthesis of methanol by hydrogenation of  $\text{CO}_2$ . The 1D quantum confinement effect leads to a larger

d band level in the RhW alloy-based nanosheet, while an electronic effect associated with the alloy mechanism results in a negatively charged Rh surface (Table 1).<sup>364</sup>

Electrochemical catalytic conversion of  $\text{CO}_2$  to methanol using precious metal catalysts is another interesting approach to  $\text{CO}_2$  reduction that can be made through the electrochemical pathway. In this regard, several electrocatalysts such as CuAu, CuPd, and AgZn were found to be excellent candidates for enhancing the  $\text{CO}$ ,  $\text{CH}_4$ , and  $\text{CH}_3\text{OH}$  productions, respectively. In addition, palladium-based electrocatalysts have not received much attention despite Pd's exceptional ability to show low overpotentials for the electrochemical reduction of  $\text{CO}_2$ . In this case, when Pd is supported on carbon (Pd/C), the C added to metals improves their different properties by making them more active because carbon materials are porous. Additionally, we can use C materials with a high surface area and good electrical conductivity to stabilize high metal loadings and

enhance the electron transfer rate in both directions (from and to) of metal catalyst sites.

Similarly, Pd/C started producing formate at 0.00 V vs. RHE, with hydrogen being the only by-product (0.00 to  $-0.20$  V vs. RHE).<sup>388</sup> So, the unwanted hydrogen evolution happens at the same time at Pd (supported on C) electrodes, along with the electrocatalytic reduction and hydrogenation of  $\text{CO}_2$  to formate. However, the combination of Pd with Zn led to the formation of formate species that remain adsorbed on the PdZn alloy surface for long enough to be converted into  $\text{CH}_3\text{OH}$ . Another interesting study on Pd-based materials was reported by Han *et al.* Herein, the Pd combined with  $\text{SnO}_2$ , forming plentiful Pd–O–Sn

interfaces, undergoes four-electron transfer mechanisms for selective  $\text{CO}_2$  reduction to methanol.<sup>389</sup> This excellent design helped to achieve a faradaic efficiency (FE) of  $54.8\% \pm 2\%$  for  $\text{CH}_3\text{OH}$  at  $-0.24$  V vs. RHE, and was able to deliver higher energy density as compared to sole Pd nanosheets (NSs) and  $\text{SnO}_2$  nanoparticles. They also reported that the current densities of Pd– $\text{SnO}_2$  NSs didn't change much, and a high FE of 54% retains over 24 hours, indicating that it is more stable. This structure not only facilitated  $\text{CO}_2$  adsorption on the  $\text{SnO}_2$  surface, but also made it difficult for CO to remain on Pd due to the Pd–O–Sn interface weakening the binding strength of CO to Pd. In turn, enhancing Pd catalysts'  $\text{CO}_2\text{RR}$  performance is

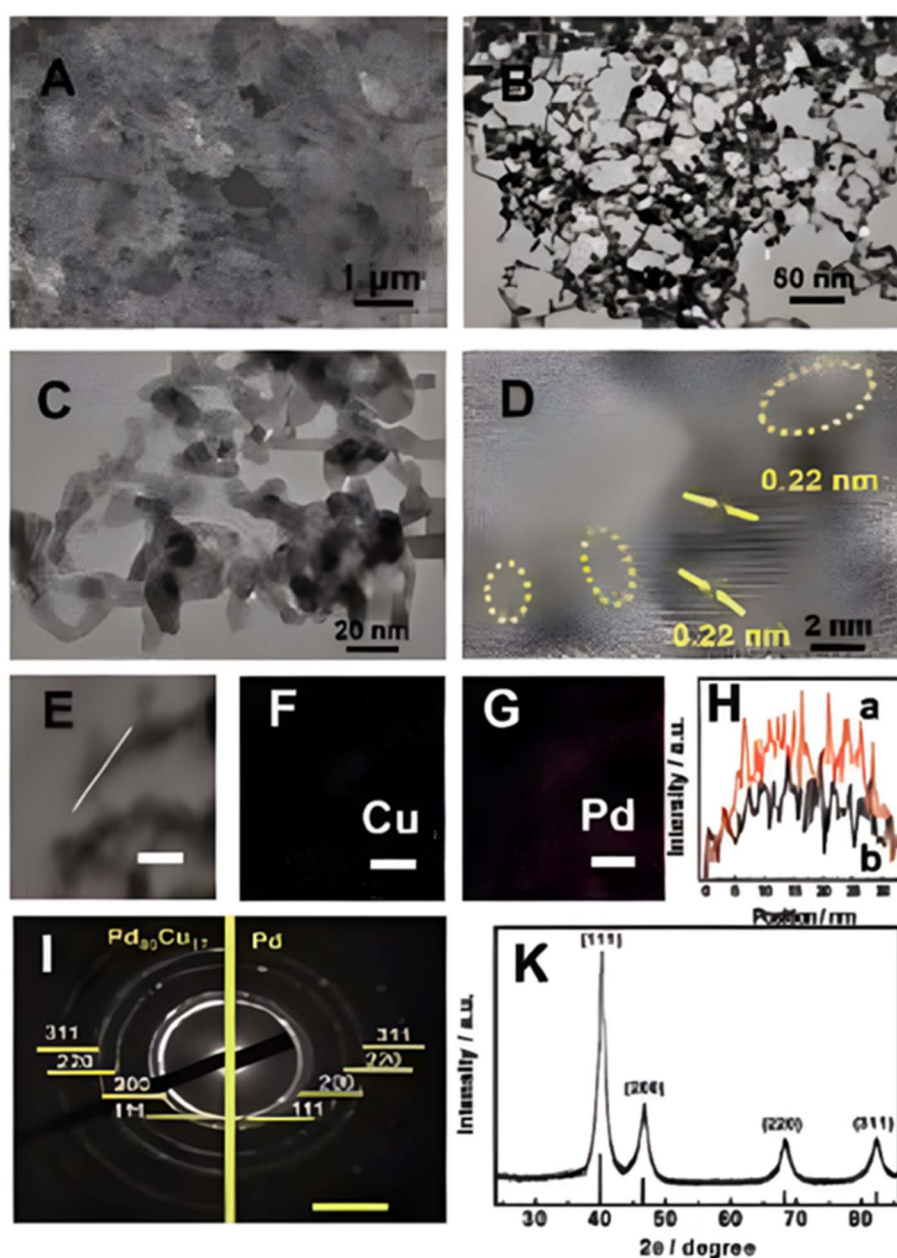


Fig. 15 (A) SEM, (B) and (C) TEM, (D) HR-TEM, and (E)–(G) EDX mapping images (scale bar: 20 nm). (H) Distribution of Pd (a) and Cu (b) in  $\text{Pd}_{83}\text{Cu}_{17}$  by line-scan analysis. (I) SAED pattern of the  $\text{Pd}_{83}\text{Cu}_{17}$  and pure Pd (scale bar: 10 nm@1). (K) XRD pattern of the  $\text{Pd}_{83}\text{Cu}_{17}$  aerogel. Reprinted with permission from ref. 389 Copyright permission from 2018 Wiley-VCH Verlag GmbH & Co. KGaA, Weinheim.

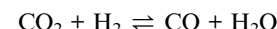


crucial in such a circumstance. Different types of electrochemical studies performed are given in Fig. 14.

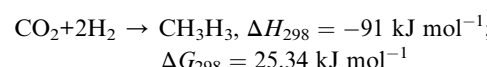
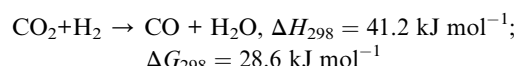
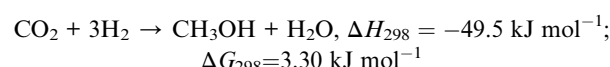
Another excellent study was carried out by Buxing Han *et al.*,<sup>389</sup> they developed a  $\text{Pd}_x\text{Cu}_y$  aerogel electrocatalyst and investigated it in a  $\text{CO}_2$ -saturated aqueous ionic liquid, 1-butyl-3-methylimidazolium tetrafluoroborate ( $[\text{Bmim}]\text{BF}_4$ ) electrolyte containing 25 mol%  $[\text{Bmim}]\text{BF}_4$  and 75 mol% water *via* a H-type cell. The characterization studies of that sample were carried out by SEM, TEM, HRTEM, SAED and XRD and the results are given in Fig. 15.

They achieved the highest Brunauer–Emmett–Teller (BET) surface area of  $76.9 \text{ m}^2 \text{ g}^{-1}$  for  $\text{Pd}_{67}\text{Cu}_{33}$  aerogels. This aerogel was capable of delivering FE efficiency for  $\text{CH}_3\text{OH}$  within the range of  $-1.9 \text{ V}$  to  $-2.4 \text{ V}$  (vs.  $\text{Ag}/\text{Ag}^+$ ). It has been found that the proportion of Cu present in the aerogel also played a crucial role in the FE of  $\text{CH}_3\text{OH}$ . In a  $[\text{Bmim}]\text{BF}_4$  aqueous solution with 25 mol%  $[\text{Bmim}]\text{BF}_4$  and 75 mol% water, the FE for  $\text{CH}_3\text{OH}$  production for  $\text{Pd}_{83}\text{Cu}_{17}$  is highest (80.0%) among others at  $-2.1 \text{ V}$  (vs.  $\text{Ag}/\text{Ag}^+$ ) after 5 hours of electrolysis. For this material, the results of the electrochemical characterization studies are given in Fig. 16.

Unlike Pd, the intermediate cannot be stabilized long enough for the reverse water-gas shift (RWGS) reaction to proceed without the intermediate first being decomposed to give CO and  $\text{H}_2\text{O}$ .<sup>320</sup>



Here, we need to discuss the RWGS process. In general, an exothermic reaction occurs during the generation of methanol from carbon dioxide using a catalytic hydrogenation process. Numerous pilot plants have used this technical method, which combines the normal methanol synthesis process with the RWGS process.



The water formation at the 2nd step inhibits the methanol synthesis through a catalytic way. Hence, the design of materials is important in which the metal's tolerance towards the water is essential. Brisard *et al.*, using differential electrochemical mass spectrometry, studied the electroreduction of carbon dioxide at a Pt porous electrode.<sup>391</sup> With their findings, it was demonstrated that a Pt electrodeposited electrode could be

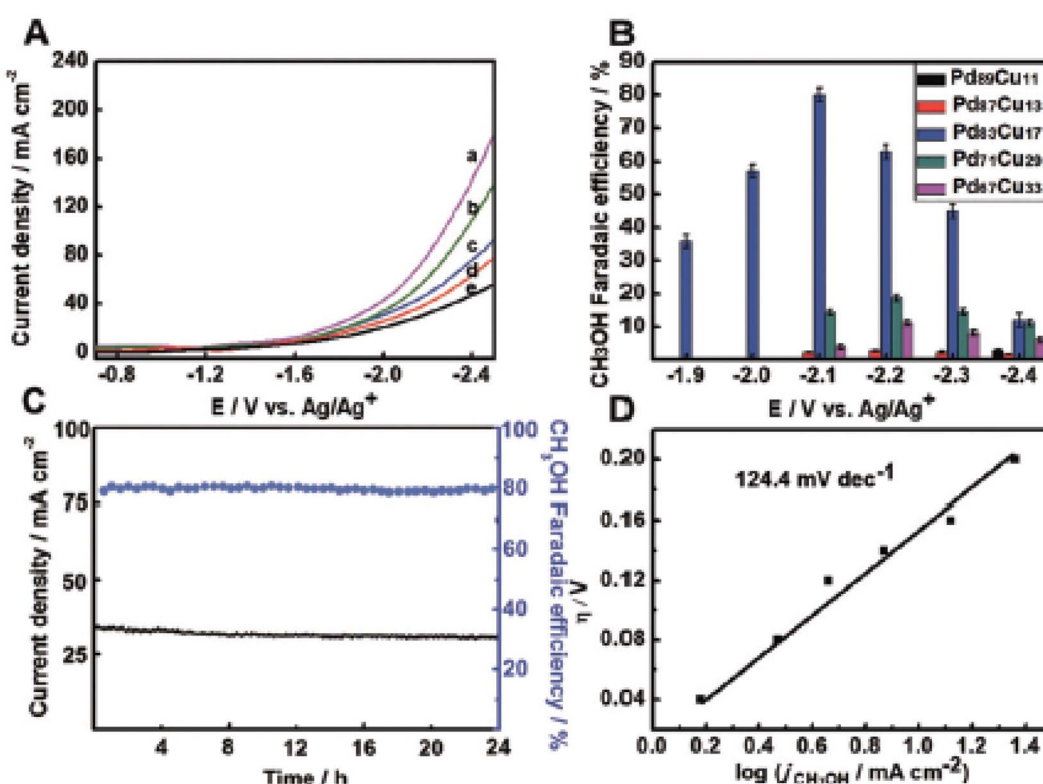


Fig. 16 The as performed  $\text{CO}_2$  electroreduction reactions in ionic liquid  $[\text{Bmim}]\text{BF}_4$  aqueous solution combined with 25 mol%  $[\text{Bmim}]\text{BF}_4$  and 75 mol% water. (A) Different LSV curves for  $\text{Pd}_x\text{Cu}_y$  aerogels are given such as: (a)  $\text{Pd}_{67}\text{Cu}_{33}$ , (b)  $\text{Pd}_{71}\text{Cu}_{29}$ , (c)  $\text{Pd}_{83}\text{Cu}_{17}$ , (d)  $\text{Pd}_{71}\text{Cu}_{13}$ , and (e)  $\text{Pd}_{89}\text{Cu}_{11}$ . (B) The FE for  $\text{CH}_3\text{OH}$  over  $\text{Pd}_x\text{Cu}_y$  aerogels. (C) Current density and FE over  $\text{Pd}_{83}\text{Cu}_{17}$  aerogel electrodes at  $@2.1 \text{ V}$  vs.  $\text{Ag}/\text{Ag}^+$ . (D) Tafel plots for  $\text{CH}_3\text{OH}$  production over  $\text{Pd}_{83}\text{Cu}_{17}$  aerogel electrodes. Reprinted with permission from ref. 389. Copyright permission from 2018 Wiley-VCH Verlag GmbH & Co. KGaA, Weinheim.



used to produce  $\text{CH}_3\text{OH}$  in the presence of acidic media. These findings further indicated that CO was formed as an intermediate leading to the production of  $\text{CH}_3\text{OH}$ . As part of efforts to develop a reversible fuel cell based on  $\text{CH}_3\text{OH}$ , Shironita *et al.* recently studied the electroreduction of  $\text{CO}_2$  on the carbon-supported Pt (Pt/C) and Pt-Ru (Pt-Ru/C) electrodes through a single cell. Faradaic efficiency estimates for the electroreduction of  $\text{CO}_2$  range from 30–50%. They concluded that the reduction current decreases over time because of the accumulation of  $\text{CH}_3\text{OH}$  on the reaction active sites of the electrocatalyst (Pt/C). This is the reason the efficiency of yielding  $\text{CH}_3\text{OH}$  went from 0.03% at Pt/C compared to 7.5% in the case of Pt-Ru/C. Also, cyclic voltammetry measurements showed that the faradaic efficiencies of Pt/C and Pt-Ru/C were 35% and 75%, respectively. In addition to having a significant impact on the selectivity, reduction mechanisms, and efficiency of the  $\text{CO}_2$  electroreduction process, the metal surface was also affected by a variety of other factors. In fact, it has been discovered that changing supporting electrolytes and operating circumstances has a significant impact on current density, product selectivity, and energy efficiency in  $\text{CO}_2$  reduction even for the same metal electrode with the same purity.<sup>392</sup>

The binding energy of the reaction intermediates on the catalyst surface affects both the catalyst's reaction activity and selectivity. During the electrochemical reduction of  $\text{CO}_2$ , a complex reaction occurs that involves multi-electron transfers and a diverse array of intermediates and products, hence it is necessary to regulate the adsorption energy of the various intermediate species that are produced. In order to modify the binding energy of intermediates for desired end products, it is rational to create specialized surface structures.

## 6. Challenges and possibilities of $\text{CO}_2$ conversion

A diverse range of problems, along with intriguing prospects, exists for the conversion of  $\text{CO}_2$  into frequently utilized formal products. Despite  $\text{CO}_2$  being a plentiful and inexpensive source, its chemical inertness frequently makes conversion procedures energy-intensive and economically impractical at large scales. Recent advancements in catalysis, electrochemistry, and process engineering are generating new opportunities for effective  $\text{CO}_2$  usage for methanol production (Fig. 17).

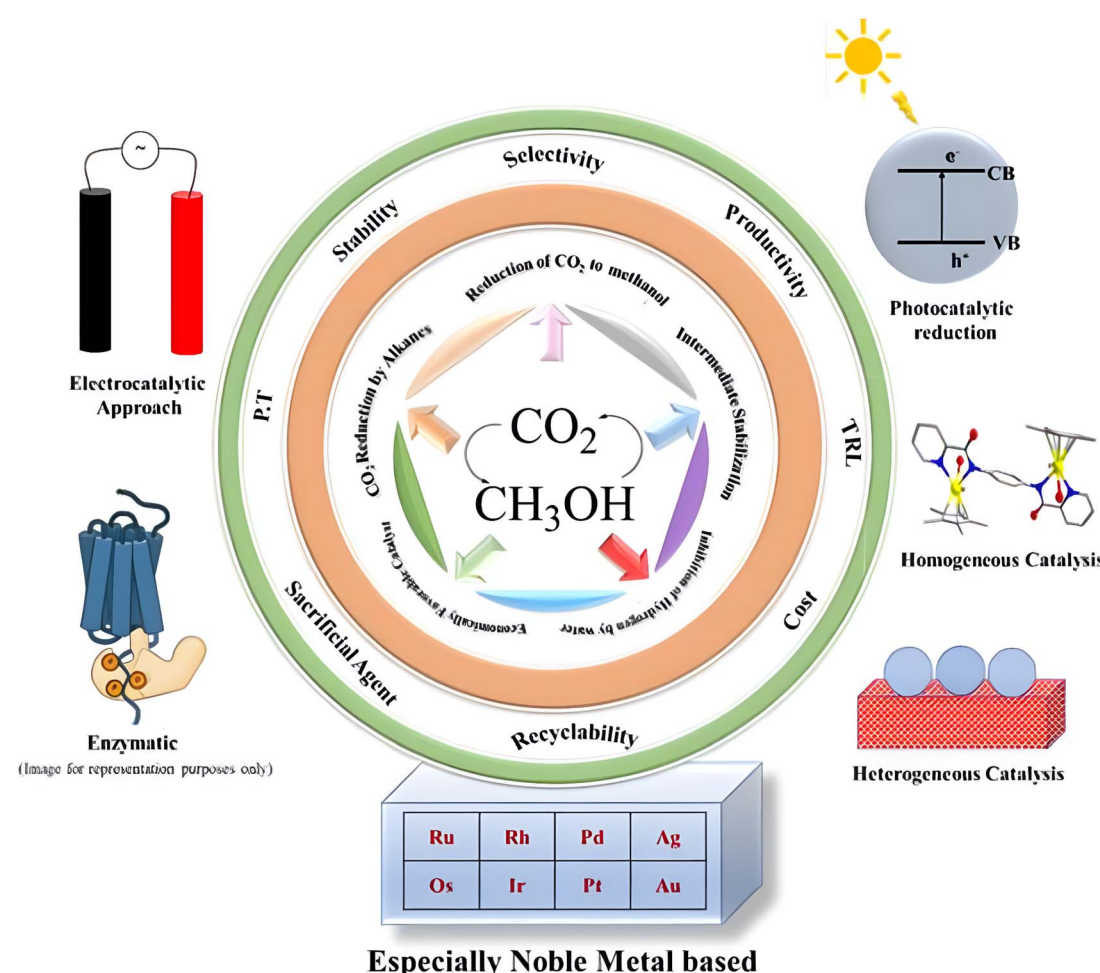


Fig. 17 Different Challenges and possibilities of  $\text{CO}_2$  to methanol conversion (with various catalysts used).



(i)  $\text{CO}_2$  is a linear, kinetically inert, nonpolar molecule with two opposite reactive sites, *i.e.*, carbonyl carbon has an electron-donating nature, and oxygen is an electron withdrawing species. Therefore, breaking the two double bonds present in the inert  $\text{CO}_2$  molecule requires a higher energy, which poses the main challenge for the reduction of  $\text{CO}_2$  to methanol.<sup>257</sup> The conversion of  $\text{CO}_2$  to CO or other value-added products is facilitated using the metal surface catalysts.<sup>258</sup>

The methanol synthesis from  $\text{CO}_2$  generates water as a byproduct, which directly influences the rapid sintering and deactivation of the Cu/ZnO catalyst. As a result, if the RWGS reaction occurs at a high temperature, it continues in an endothermic mode, and if it occurs at a lower temperature, it reduces the catalytic activity, which can be considered the main drawback of  $\text{CO}_2$ .<sup>69,259,260</sup>

#### (ii) Intermediate stabilization

In methanol synthesis from the hydrogenation of  $\text{CO}_2$ , controlling the intermediate stabilization is another critical challenge. CO is a crucial intermediate in the catalytic hydrogenation of methanol synthesis. From a thermodynamic perspective, the bonding between CO and the catalyst surface develops a stronger binding energy that increases the reaction rate of methanol or any other hydrocarbon synthesis process, while the bonding between the catalyst surface and CO initiates the RWGS reaction with weaker binding energy.<sup>261</sup> For methanol synthesis, controlling the stabilization of the intermediate, *i.e.*, CO, is crucial for increasing the yields.<sup>123</sup> DFT calculations and studies reveal that multiple factors influence catalytic properties. These include the key intermediate, oxygen adsorption energy, the relationship between catalyst structure and properties, and  $\text{CO}_2$  adsorption phenomena. This understanding provides a novel approach for catalyst development.<sup>393</sup>

#### (iii) Inhibition of hydrogenation by water

The production of large amounts of water during the reduction of  $\text{CO}_2$  by  $\text{H}_2$  reduces the catalytic activity of the catalyst through the formation of hydroxyl. The main challenge of researchers is to develop a hydrothermal catalyst that resists catalyst poisoning. However, some research groups improved the catalytic activity of methanol production from  $\text{CO}_2$  by using promising noble metals, primarily Pd, Pt-based microporous  $\text{SiO}_2$ -supported catalysts, and carbon shell-supported catalysts.<sup>394,395</sup>

#### (iv) Development of economically favorable catalysts

One of the challenges researchers face is developing a low-cost, economically advantageous catalyst with good recycling and reducible qualities that would produce large amounts of methanol from the  $\text{CO}_2$  hydrogenation process.<sup>396</sup> Recently, some research groups developed a  $\text{Mo}_2\text{C}$  catalyst; however, this catalyst's main disadvantage is coke formation because, during the reaction, it binds firmly to intermediate hydrocarbons.<sup>397</sup>

#### (v) $\text{CO}_2$ reduction by alkanes

Researchers are trying to develop an alternative path for the reduction of  $\text{CO}_2$ . An alternate substance that can be used to reduce  $\text{CO}_2$  might be light alkanes.<sup>398</sup> Although methane dry reforming can be employed as an alternative to hydrogen gas, researchers have observed that the catalyst rapidly loses effectiveness when exposed to elevated temperatures. But in the case of ethane, thermodynamically favorable conditions are

available for  $\text{CO}_2$  hydrogenation. In the near future, one of the hotspot research topics for energy engineering would be  $\text{CO}_2$  reduction *via* light alkanes.<sup>389</sup>

## 7. Conclusion & future perspectives

This review emphasizes the use of noble metal-based catalysts for the hydrogenation of  $\text{CO}_2$  to produce methanol. It is evident that several aspects of catalysts are important including promoters, support types, synthetic procedures, reaction circumstances, large surface area, and particle size, all of which must be taken into consideration to design catalysts to achieve higher performance.

The "Methanol Economy" offers a promising strategy for addressing global warming by utilizing  $\text{CO}_2$  as a renewable energy resource. Methanol can serve as an energy storage medium, hydrocarbon feedstock, and alternative fuel. Various catalysts, including those based on noble metals, have been developed for the hydrogenation of methanol from  $\text{CO}_2$ . The conversion of  $\text{CO}_2$  to methanol using heterogeneous and electrochemical catalysts holds industrial promise but faces significant challenges. Heterogeneous catalysts, such as noble metal-based systems, are advantageous due to ease of separation and recyclability but are hindered by mass transport and diffusion limitations. Electrochemical catalysts offer high selectivity and efficiency but require precise control of operating conditions and are sensitive to electrode materials and electrolytes. Nanostructured catalysts can enhance surface area and tunability, improving reaction rates and stability. However, scaling these technologies from lab to industry involves challenges in reactor design, mass transport, and heat management, essential for commercial viability. Addressing these issues is crucial for the success of  $\text{CO}_2$  to methanol conversion technologies. The procedure's efficacy depends on understanding fundamental chemistry, catalyst characterization, and reactor characteristics. Researchers aim to develop dual-function promoters to improve  $\text{CO}_2$  to  $\text{CH}_3\text{OH}$  conversion and reduce CO *via* the RWGS reaction. While noble metal-based catalysts show exceptional efficacy, their limited activity and high cost make them economically impractical. To commercialize  $\text{CO}_2$ -derived methanol synthesis, researchers need to integrate multiple elements into a single material or process. This may involve creating innovative materials that combine the catalytic abilities of noble metals with more abundant and cost-effective components, enhancing efficiency and reducing costs. Additionally, improving reactor designs to increase  $\text{CO}_2$ -catalyst interaction could further boost conversion rates and overall feasibility.

The hydrogenation of  $\text{CO}_2$  to methanol, despite its limitations, offers promising pathways for sustainable fuel production. Although progress has been made in understanding reaction mechanisms and catalyst design, critical areas still require further research. This study establishes a foundation for sustainable fuel production methods, potentially reducing fossil fuel dependence. By identifying key areas for future research, it paves the way for advances in  $\text{CO}_2$  utilization and catalyst design, which could significantly impact climate



change mitigation and the shift to sustainable energy. Priority areas include developing low-temperature reactive catalysts, optimizing reaction conditions and reactor designs, and employing guided rational catalyst design and synthesis. Future efforts may utilize advanced analytical techniques and computational methods to further elucidate reaction mechanisms. Bridging the gap between model catalysts and industrial-scale processing remains crucial for commercialization. The field shows promise through the development of novel materials, particularly noble metal-based catalysts, and the exploration of energy-efficient technologies. Ultimately, achieving sustainable methanol production from CO<sub>2</sub> hydrogenation will necessitate interdisciplinary collaboration and innovative strategies to overcome existing challenges, contributing significantly to global initiatives aimed at reducing atmospheric CO<sub>2</sub>.

## Data availability

No primary research results, software or code have been included and no new data were generated or analysed as part of this review.

## Author contributions

Soumalya Roy: conceptualization, investigation, data generation, and writing—original draft. Ezhava Manu Manohar: administration and data validation. Dr Sujoy Bandyopadhyay: administration and data validation. Dr Manik Chandra Singh: administration and data validation. Yeji Cha: administration and data validation. Dr Soumen Giri: writing and editing. Dr Sharad Lande: writing and editing. Dr Kyungsu Na: conceptualization, result validation, supervision, writing, editing, and methodology. Dr Junseong Lee: conceptualization, result validation, supervision, writing, editing, and methodology. Dr Sourav Das: conceptualization, result validation, supervision, writing, editing, and methodology.

## Conflicts of interest

The authors declare no competing financial interest.

## Acknowledgements

The authors express their gratitude to the Institute of Infrastructure Technology Research & Management (IITRAM, Ahmedabad), Reliance Industries Limited, and C. V. Raman Global University. J. L. acknowledges the financial support from the National Research Foundation of Korea (NRF) grant funded by the Korean government (RS-2023-00218219 and 2022R1A2C100611312) and the 'Regional Innovation Strategy (RIS)' through the National Research Foundation of Korea (NRF), funded by the Ministry of Education (MOE) (2021RIS-002). S. B. is thankful for the financial support provided by the National Research Foundation of Korea (NRF) grant funded by the Korea government Ministry of Science and NRF BP (Project Number RS-2023-00263849).

## References

- 1 M. E. Boot-Handford, J. C. Abanades, E. J. Anthony, M. J. Blunt, S. Brandani, N. Mac Dowell, J. R. Fernández, M.-C. Ferrari, R. Gross and J. P. Hallett, *Energy Environ. Sci.*, 2014, **7**, 130–189.
- 2 J. Chen, M. J. Dahlin, L. Luuppala, D. Bickford, L. Boljka, V. Burns and M. S. Johnson, *Nature*, 2021, 279–325.
- 3 IEA, *Defying Expectations, CO<sub>2</sub> Emissions from Global Fossil Fuel Combustion are Set to Grow in 2022 by Only a Fraction of Last Year's Big Increase*, 2022, <https://www.iea.org/news/defying-expectations-co2-emissions-from-global-fossil-fuel-combustion-are-set-to-grow-in-2022-by-only-a-fraction-of-last-year-s-big-increase>.
- 4 S. Seneviratne, N. Nicholls, D. Easterling, C. Goodess, S. Kanae, J. Kossin, Y. Luo, J. Marengo, K. McInnes, M. Rahimi, M. Reichstein, A. Sorteberg, C. Vera and X. Zhang, Changes in climate extremes and their impacts on the natural physical environment, in *Managing the Risks of Extreme Events and Disasters to Advance Climate Change Adaptation: A Special Report of Working Groups I and II of the Intergovernmental Panel on Climate Change (IPCC)*, ed. C. B. Field, V. Barros, T. F. Stocker, D. Qin, D. J. Dokken, K. L. Ebi, M. D. Mastrandrea, K. J. Mach, G.-K. Plattner, S. K. Allen, M. Tignor and P. M. Midgley, Cambridge University Press, Cambridge, UK, New York, NY, USA, 2012, pp. 109–230.
- 5 O. Hoegh-Guldberg, D. Jacob, M. Bind, S. Brown, I. Camilloni, A. Diedhiou, R. Djalante, K. Ebi, F. Engelbrecht and J. Guiot, *Global Warming of 1.5 °C*, 2018.
- 6 J. Hansen, M. Sato, R. Ruedy, K. Lo, D. W. Lea and M. Medina-Elizade, *Proc. Natl. Acad. Sci. U. S. A.*, 2006, **103**, 14288–14293.
- 7 B. Soergel, E. Kriegler, I. Weindl, S. Rauner, A. Dirnachner, C. Ruhe, M. Hofmann, N. Bauer, C. Bertram and B. L. Bodirsky, *Nat. Clim. Change*, 2021, **11**, 656–664.
- 8 G. A. Olah, G. S. Prakash and A. Goepert, *J. Am. Chem. Soc.*, 2011, **133**, 12881–12898.
- 9 G. Flato, J. Marotzke, B. Abiodun, P. Braconnat, S. C. Chou, W. Collins, P. Cox, F. Driouech, S. Emori and V. Eyring, in *Climate Change 2013: the Physical Science Basis. Contribution of Working Group I to the Fifth Assessment Report of the Intergovernmental Panel on Climate Change*, Cambridge University Press, 2014, pp. 741–866.
- 10 M. He, Y. Sun and B. Han, *Angew. Chem., Int. Ed.*, 2013, **52**, 9620–9633.
- 11 P. Nema, S. Nema and P. Roy, *Renewable Sustainable Energy Rev.*, 2012, **16**, 2329–2336.
- 12 J. A. Patz, M. L. Grabow and V. S. Limaye, *Ann. Glob. Health*, 2014, **80**, 332–344.
- 13 A. Mikhaylov, N. Moiseev, K. Aleshin and T. Burkhardt, *Entrep., Sustain. Issues*, 2020, **7**, 2897.
- 14 N. Linares, A. M. Silvestre-Albero, E. Serrano, J. Silvestre-Albero and J. García-Martínez, *Chem. Soc. Rev.*, 2014, **43**, 7681–7717.
- 15 J. J. Spivey, *Catal.*, 2005, **100**, 171–180.



16 L. Grandell, A. Lehtilä, M. Kivinen, T. Koljonen, S. Kihlman and L. S. Lauri, *Renewable Energy*, 2016, **95**, 53–62.

17 S. Perathoner and G. Centi, *ChemSusChem*, 2014, **7**, 1274–1282.

18 E. A. Quadrelli, G. Centi, J. L. Duplan and S. Perathoner, *ChemSusChem*, 2011, **4**, 1194–1215.

19 S. Perathoner, K. M. Van Geem, G. B. Marin and G. Centi, *ChemComm.*, 2021, **57**, 10967–10982.

20 S. Carley and D. M. Konisky, *Nat. Energy*, 2020, **5**, 569–577.

21 W. Wang, S. Wang, X. Ma and J. Gong, *Chem. Soc. Rev.*, 2011, **40**, 3703–3727.

22 M. Ding, R. W. Flaig, H.-L. Jiang and O. M. Yaghi, *Chem. Soc. Rev.*, 2019, **48**, 2783–2828.

23 X. Jiang, X. Nie, X. Guo, C. Song and J. G. Chen, *Chem. Rev.*, 2020, **120**, 7984–8034.

24 W. Gao, S. Liang, R. Wang, Q. Jiang, Y. Zhang, Q. Zheng, B. Xie, C. Y. Toe, X. Zhu and J. Wang, *Chem. Soc. Rev.*, 2020, **49**, 8584–8686.

25 O. Hoegh-Guldberg and J. F. Bruno, *Science*, 2010, **328**, 1523–1528.

26 K. Lee, H. Yan, Q. Sun, Z. Zhang and N. Yan, *Acc. Mater. Res.*, 2023, **4**, 746–757.

27 S. Valluri, V. Claremboux and S. Kawatra, *J. Environ. Sci.*, 2022, **113**, 322–344.

28 Z. Zhang, S.-Y. Pan, H. Li, J. Cai, A. G. Olabi, E. J. Anthony and V. Manovic, *Renew. Sustain. Energy Rev.*, 2020, **125**, 109799.

29 Z. Zhang, S.-Y. Pan, H. Li, J. Cai, A. G. Olabi, E. J. Anthony and V. Manovic, *Renew. Sustain. Energy Rev.*, 2020, **125**, 109799.

30 T. Wilberforce, A. Olabi, E. T. Sayed, K. Elsaid and M. A. Abdelkareem, *Sci. Total Environ.*, 2021, **761**, 143203.

31 N. Zhu, Y. Liu, L. Yang, C. Jiang and N. Wei, *Renew. Sustain. Energy Rev.*, 2025, **207**, 114899.

32 J. Ma, L. Li, H. Wang, Y. Du, J. Ma, X. Zhang and Z. Wang, *Engineering*, 2022, **14**, 33–43.

33 S. Paltsev, J. Morris, H. Kheshgi and H. Herzog, *Appl. Energy*, 2021, **300**, 117322.

34 T. Kazlou, A. Cherpi and J. Jewell, *Nat. Clim. Change*, 2024, **1**–9.

35 L. Rosa, D. L. Sanchez, G. Realmonte, D. Baldocchi and P. D'Odorico, *Renew. Sustain. Energy Rev.*, 2021, **138**, 110511.

36 E. S. Sanz-Pérez, C. R. Murdock, S. A. Didas and C. W. Jones, *Chem. Rev.*, 2016, **116**, 11840–11876.

37 A. Sodiq, Y. Abdullatif, B. Aissa, A. Ostovar, N. Nassar, M. El-Naas and A. Amhamed, *Environ. Technol. Innov.*, 2023, **29**, 102991.

38 X. Shi, H. Xiao, H. Azarabadi, J. Song, X. Wu, X. Chen and K. S. Lackner, *Angew. Chem. Int. Ed.*, 2020, **59**, 6984–7006.

39 M. Erans, E. S. Sanz-Pérez, D. P. Hanak, Z. Clulow, D. M. Reiner and G. A. Mutch, *Energy Environ. Sci.*, 2022, **15**, 1360–1405.

40 X. Zhu, W. Xie, J. Wu, Y. Miao, C. Xiang, C. Chen, B. Ge, Z. Gan, F. Yang and M. Zhang, *Chem. Soc. Rev.*, 2022, **51**, 6574–6651.

41 D. Fu and M. E. Davis, *Chem. Soc. Rev.*, 2022, **51**, 9340–9370.

42 H. Li, A. Dilipkumar, S. Abubakar and D. Zhao, *Chem. Soc. Rev.*, 2023, **52**, 6294–6329.

43 R. Castro-Munoz, M. Z. Ahmad, M. Malankowska and J. Coronas, *J. Chem. Eng.*, 2022, **446**, 137047.

44 J. Wang, R. Fu, S. Wen, P. Ning, M. H. Helal, M. A. Salem, B. B. Xu, Z. M. El-Bahy, M. Huang and Z. Guo, *Adv. Compos. Hybrid Mater.*, 2022, **5**, 2721–2759.

45 M. Ding, X. Liu, P. Ma and J. Yao, *Coord. Chem. Rev.*, 2022, **465**, 214576.

46 C. Xiao, J. Tian, Q. Chen and M. Hong, *Chem. Sci.*, 2024, **15**, 1570–1610.

47 L. James, *From Capture to Storage: Understanding the Viability and Challenges of Carbon Capture and Sequestration Initiatives*, Massachusetts Institute of Technology, 2024.

48 H. Herzog, *Environ. Sci. Technol.*, 2001, **35**, 148A.

49 E. Martin-Roberts, V. Scott, S. Flude, G. Johnson, R. S. Haszeldine and S. Gilfillan, *One Earth*, 2021, **4**, 1569–1584.

50 T. M. Gür, *Prog. Energy Combust. Sci.*, 2022, **89**, 100965.

51 M. Bui, C. S. Adjiman, A. Bardow, E. J. Anthony, A. Boston, S. Brown, P. S. Fennell, S. Fuss, A. Galindo and L. A. Hackett, *Energy Environ. Sci.*, 2018, **11**, 1062–1176.

52 R. L. Siegelman, E. J. Kim and J. R. Long, *Nat. Mater.*, 2021, **20**, 1060–1072.

53 S. Deutz and A. Bardow, *Nat. Energy*, 2021, **6**, 203–213.

54 B. Dziejarski, R. Krzyżynska and K. Andersson, *Fuel*, 2023, **342**, 127776.

55 H. Liu, C. Consoli and A. Zapantis, Overview of Carbon Capture and Storage (CCS) facilities globally, in *14th Greenhouse Gas Control Technologies Conference Melbourne*, 2018, pp. 1–10.

56 A. Olabi, T. Wilberforce, K. Elsaid, E. T. Sayed, H. M. Maghrabie and M. A. Abdelkareem, *J. Clean. Prod.*, 2022, **362**, 132300.

57 N. Darraj, M. M. Abdelrahman and M. Y. Alklih, *Regional Review for Large-Scale Deployment of Carbon Capture and Storage (CCS) in the Middle East*, 2024.

58 D. Cha, *Australian Energy Producers Journal*, 2024, **64**, S119–S124.

59 A. E. Ikpe, I. Ekanem and K. R. Ekanem, *Int. J. Energy Environ. Eng.*, 2024, **1**, 1–15.

60 J. Li, C. Zhang, M. R. Davidson and X. Lu, *Appl. Energy*, 2025, **377**, 124459.

61 O. Massarweh and A. S. Abushaikha, *Petroleum*, 2022, **8**, 291–317.

62 L. W. Lake, R. Johns, B. Rossen and G. A. Pope, *Fundamentals of Enhanced Oil Recovery*, Society of Petroleum Engineers, Richardson, TX, 2014.

63 S. Davoodi, M. Al-Shargabi, D. A. Wood, M. Mehrad and V. S. Rukavishnikov, *Fuel*, 2024, **366**, 131313.

64 E. S. Rubin, J. E. Davison and H. J. Herzog, *Int. J. Greenhouse Gas Control*, 2015, **40**, 378–400.

65 J. Rissman, C. Bataille, E. Masanet, N. Aden, W. R. Morrow III, N. Zhou, N. Elliott, R. Dell, N. Heeren and B. Hückestein, *Appl. Energy*, 2020, **266**, 114848.



66 G. Brändle, M. Schönfisch and S. Schulte, *Appl. Energy*, 2021, **302**, 117481.

67 J. A. Garcia, M. Villen-Guzman, J. M. Rodriguez-Maroto and J. M. Paz-Garcia, *J. Environ. Chem. Eng.*, 2022, **10**, 108470.

68 S. Griffiths, B. K. Sovacool, J. Kim, M. Bazilian and J. M. Uratani, *Energy Res. Soc. Sci.*, 2021, **80**, 102208.

69 A. Mirzaei-Paiaman, R. Okuno, T. Lawal, K. Sheng, C. Chen, I. Lai, S. Chen and L. Hu, *Techno-Economic-Environmental Analysis of CO<sub>2</sub> Storage and EOR in an Underdeveloped Field*, 2024.

70 P. Roefs, M. Moretti, K. Welkenhuysen, K. Piessens and T. Compernolle, *J. Environ. Manag.*, 2019, **239**, 167–177.

71 X. Yao, P. Zhong, X. Zhang and L. Zhu, *Energy Pol.*, 2018, **121**, 519–533.

72 X. Wu, Z. Tian and J. Guo, *Sustain. Oper. Comput.*, 2022, **3**, 54–66.

73 B. Lin and Z. Tan, *J. Clean. Prod.*, 2021, **298**, 126768.

74 A. Al-Mamoori, A. Krishnamurthy, A. A. Rownaghi and F. Rezaei, *Energy Technol.*, 2017, **5**, 834–849.

75 T. Wilberforce, A. Baroutaji, B. Soudan, A. H. Al-Alami and A. G. Olabi, *Sci. Total Environ.*, 2019, **657**, 56–72.

76 J. C. Pires, F. G. Martins, M. C. Alvim-Ferraz and M. Simões, *Chem. Eng. Res. Des.*, 2011, **89**, 1446–1460.

77 A. I. Osman, M. Hefny, M. Abdel Maksoud, A. M. Elgarahy and D. W. Rooney, *Environ. Chem. Lett.*, 2021, **19**, 797–849.

78 M. L. Szulczewski, C. W. MacMinn, H. J. Herzog and R. Juanes, *Proc. Natl. Acad. Sci. U. S. A.*, 2012, **109**, 5185–5189.

79 R. Wennersten, Q. Sun and H. Li, *J. Clean. Prod.*, 2015, **103**, 724–736.

80 Y.-M. Wei, J.-N. Kang, L.-C. Liu, Q. Li, P.-T. Wang, J.-J. Hou, Q.-M. Liang, H. Liao, S.-F. Huang and B. Yu, *Nat. Clim. Change*, 2021, **11**, 112–118.

81 J. Ladenburg, J. Kim, M. Zuch and U. Soytas, *Renewable Energy*, 2024, **220**, 119582.

82 J. Rowland, S. López-Asensio, A. Bagci, A. Delicado and A. Prades, *J. Assoc. Inf. Sci. Technol.*, 2024, **75**, 625–639.

83 G. A. Olah, G. S. Prakash and A. Goeppert, *J. Am. Chem. Soc.*, 2011, **133**, 12881–12898.

84 Z. Caineng, B. Xiong, X. Huaqing, D. Zheng, G. Zhixin, W. Ying, L. Jiang, P. Songqi and W. Songtao, *Petrol. Explor. Dev.*, 2021, **48**, 480–491.

85 R. M. Andrew, *Earth Syst. Sci. Data*, 2020, **12**, 1437–1465.

86 H. Ritchie and M. Roser, *Our World in Data*, 2024.

87 S. J. Davis and K. Caldeira, *Proc. Natl. Acad. Sci. U. S. A.*, 2010, **107**, 5687–5692.

88 Z. Wang and X. Jia, *Energy Rep.*, 2022, **8**, 1667–1679.

89 S. Saeidi, N. A. S. Amin and M. R. Rahimpour, *J. CO<sub>2</sub> Util.*, 2014, **5**, 66–81.

90 S. Saeidi, S. Najari, V. Hessel, K. Wilson, F. J. Keil, P. Concepción, S. L. Suib and A. E. Rodrigues, *Prog. Energy Combust. Sci.*, 2021, **85**, 100905.

91 Z. Hua, Y. Yang and J. Liu, *Coord. Chem. Rev.*, 2023, **478**, 214982.

92 M. Aktary, H. S. Alghamdi, A. M. Ajeebi, A. S. AlZahrani, M. A. Sanhoob, M. A. Aziz and M. Nasiruzzaman Shaikh, *Chem.-Asian J.*, 2024, e202301007.

93 N. Yusuf, F. Almomani and H. Qiblawey, *Fuel*, 2023, **345**, 128178.

94 S. Saeidi, S. Najari, F. Fazlollahi, M. K. Nikoo, F. Sefidkon, J. J. Klemeš and L. L. Baxter, *Renew. Sustain. Energy Rev.*, 2017, **80**, 1292–1311.

95 G. Wang, J. Chen, Y. Ding, P. Cai, L. Yi, Y. Li, C. Tu, Y. Hou, Z. Wen and L. Dai, *Chem. Soc. Rev.*, 2021, **50**, 4993–5061.

96 M. Alias, S. Kamarudin, A. Zainoodin and M. Masdar, *Int. J. Hydrogen Energy*, 2020, **45**, 19620–19641.

97 Y. Liu, F. M. Kirchberger, S. Müller, M. Eder, M. Tonigold, M. Sanchez-Sanchez and J. A. Lercher, *Nat. Commun.*, 2019, **10**, 1462.

98 M. Bertau, H. Offermanns, L. Plass, F. Schmidt and H.-J. Wernicke, *Methanol: the Basic Chemical and Energy Feedstock of the Future*, Springer, 2014.

99 G. A. Olah, *Angew. Chem.*, 2005, **44**, 2636–2639.

100 M. Nouni, P. Jha, R. Sarkhel, C. Banerjee, A. K. Tripathi and J. Manna, *Fuel*, 2021, **305**, 121583.

101 A. Goldmann, W. Sauter, M. Oettinger, T. Kluge, U. Schröder, J. R. Seume, J. Friedrichs and F. Dinkelacker, *Energies*, 2018, **11**, 392.

102 P. Su-Ungkavatin, L. Tiruta-Barna and L. Hamelin, *Prog. Energy Combust. Sci.*, 2023, **96**, 101073.

103 A. Goeppert, M. Czaun, G. S. Prakash and G. A. Olah, *Energy Environ. Sci.*, 2012, **5**, 7833–7853.

104 International Energy Agency (IEA), *Technology Roadmap: Delivering Sustainable Bioenergy*, IEA, Paris, France, 2017.

105 M. Fasihi and C. Breyer, *Energy Environ. Sci.*, 2024, **17**, 3503–3522.

106 S. S. Tabibian and M. Sharifzadeh, *Renew. Sustain. Energy Rev.*, 2023, **179**, 113281.

107 H.-V. Tran, T. T. Dang, N. H. Nguyen, H. T. Tran, D. T. Nguyen, D. V. Do, T. S. Le, T. H. Ngo, Y. K. Late and P. N. Amaniampong, *ChemSusChem*, 2024, e202401974.

108 J. Bao, G. Yang, Y. Yoneyama and N. Tsubaki, *ACS Catal.*, 2019, **9**, 3026–3053.

109 W. Zhang, M. Song, Q. Yang, Z. Dai, S. Zhang, F. Xin, W. Dong, J. Ma and M. Jiang, *Biotechnol. Biofuels*, 2018, **11**, 1–11.

110 G. Garcia, E. Arriola, W.-H. Chen and M. D. De Luna, *Energy*, 2021, **217**, 119384.

111 T. Klein: *Methanol: A Future-Proof Fuel A Primer Prepared for the Methanol Institute*, Methanol Institute, Alexandria, VA, USA, 2020.

112 N. Onishi and Y. Himeda, *Coord. Chem. Rev.*, 2022, **472**, 214767.

113 M. Saito, M. Takeuchi, T. Fujitani, J. Toyir, S. Luo, J. Wu, H. Mabuse, K. Ushikoshi, K. Mori and T. Watanabe, *Appl. Organomet. Chem.*, 2000, **14**, 763–772.

114 N. Onishi and Y. Himeda, *Chem Catal.*, 2021, **2**, 242–251.

115 K. Klier, in *Advances in Catalysis*, Elsevier, 1982, vol. 31, pp. 243–313.

116 S. Barman, A. Singh, F. A. Rahimi and T. K. Maji, *J. Am. Chem. Soc.*, 2021, **143**, 16284–16292.

117 S. Dang, H. Yang, P. Gao, H. Wang, X. Li, W. Wei and Y. Sun, *Catal.*, 2019, **330**, 61–75.



118 J. Strunk, K. Kähler, X. Xia and M. Muhler, *Surf. Sci.*, 2009, **603**, 1776–1783.

119 X. Chang, X. Han, Y. Pan, Z. Hao, J. Chen, M. Li, J. Lv and X. Ma, *Ind. Eng. Chem. Res.*, 2022.

120 J.-L. Dubois, K. Sayama and H. Arakawa, *Chem. Lett.*, 1992, **21**, 5–8.

121 Y. Kim, S. Kwon, Y. Song and K. Na, *J. CO<sub>2</sub> Util.*, 2020, **36**, 145–152.

122 V. Bressi, T. Len, S. Abate, C. Espro and R. Luque, *Chem. Eng. J.*, 2024, **485**, 149989.

123 F. Zhang, B. Li, X. Quan, K. Wang, J. Xu, T. Wu, Z. Li, M. Yan, S. Liu and Y. He, *ACS Catal.*, 2024, **14**, 7136–7148.

124 Q. Lu, J. Rosen, Y. Zhou, G. S. Hutchings, Y. C. Kimmel, J. G. Chen and F. Jiao, *Nat. Commun.*, 2014, **5**, 3242.

125 B. P. Sullivan, K. Krist and H. Guard, *Electrochemical and Electrocatalytic Reactions of Carbon Dioxide*, Elsevier, 2012.

126 W.-H. Wang, Y. Himeda, J. T. Muckerman, G. F. Manbeck and E. Fujita, *Chem. Rev.*, 2015, **115**, 12936–12973.

127 D. Johnson, Z. Qiao and A. Djire, *ACS Appl. Energy Mater.*, 2021, **4**, 8661–8684.

128 L. Li, X. Li, Y. Sun and Y. Xie, *Chem. Soc. Rev.*, 2022, **51**, 1234–1252.

129 H. Lee, N. Park, T.-H. Kong, S. Kwon, S. Shin, S. G. Cha, E. Lee, J. Cha, S. Sultan and Y. Kwon, *Nano Energy*, 2024, **130**, 110099.

130 X. Zhang, S.-X. Guo, K. A. Gandionco, A. M. Bond and J. Zhang, *Mater. Today Adv.*, 2020, **7**, 100074.

131 P. Saha, S. Amanullah and A. Dey, *Acc. Chem. Res.*, 2022, **55**, 134–144.

132 P. Sun, S. Liu, X. Zheng, G. Hu, Q. Zhang, X. Liu, G. Zheng and Y. Chen, *Nano Today*, 2024, **55**, 102152.

133 R. Aziz, S. Abad and S. A. Onaizi, *Chemosphere*, 2024, 143312.

134 W. Cheng, L. Sun, X. He and L. Tian, *Dalton Trans.*, 2022, **51**, 7763–7774.

135 A. Al Harthi, M. Al Abri, H. A. Younus and R. Al Hajri, *J. CO<sub>2</sub> Util.*, 2024, **83**, 102819.

136 A. Sheppard, V. Del Angel Hernandez, C. F. Faul and D. J. Fermin, *Chemelectrochem*, 2023, **10**, e202300068.

137 K. Wiranarongkorn, K. Eamsiri, Y.-S. Chen and A. Arpornwichanop, *J. CO<sub>2</sub> Util.*, 2023, **71**, 102477.

138 A. Roy, H. S. Jadhav, S. J. Park and J. G. Seo, *J. Alloys Compd.*, 2021, **887**, 161449.

139 Z. W. Seh, J. Kibsgaard, C. F. Dickens, I. Chorkendorff, J. K. Nørskov and T. F. Jaramillo, *Science*, 2017, **355**, eaad4998.

140 Z. Guo, P. Zhou, L. Jiang, S. Liu, Y. Yang, Z. Li, P. Wu, Z. Zhang and H. Li, *Adv. Mater.*, 2024, **36**, 2311149.

141 M. Zhou, Y. Zhang, H. Li, Z. Li, S. Wang, X. Lu and S. Yang, *Angew. Chem. Int. Ed.*, 2024, e202414392.

142 G. C. Chinchen, P. Denny, J. Jennings, M. Spencer and K. Waugh, *Appl. Catal.*, 1988, **36**, 1–65.

143 Q. Zhu, *Clean Energy*, 2019, **3**, 85–100.

144 C. Feliciano-Bruzual, *J. Mater. Res. Technol.*, 2014, **3**, 233–243.

145 L. Spadaro, F. Arena and A. Palella, in *Methanol*, Elsevier, 2018, pp. 429–472.

146 S. Chakrabortty, J. Nayak, B. Ruj, P. Pal, R. Kumar, S. Banerjee, M. Sardar and P. Chakraborty, *Environ. Chem. Eng.*, 2020, **8**, 103935.

147 O. Martin, A. J. Martín, C. Mondelli, S. Mitchell, T. F. Segawa, R. Hauert, C. Drouilly, D. Curulla-Ferré and J. Pérez-Ramírez, *Angew. Chem.*, 2016, **55**, 6261–6265.

148 T. Kobayashi and H. Takahashi, *Energy Fuels*, 2004, **18**, 285–286.

149 W. Sheng, S. Kattel, S. Yao, B. Yan, Z. Liang, C. J. Hawhurst, Q. Wu and J. G. Chen, *Energy Environ. Sci.*, 2017, **10**, 1180–1185.

150 J. M. Spurgeon, N. Theaker, C. A. Phipps, S. S. Uttarwar and C. A. Grapperhaus, *ACS Sustain. Chem. Eng.*, 2022, **10**, 12882–12894.

151 A. A. Kiss, J. Pragt, H. Vos, G. Bargeman and M. De Groot, *Chem. Eng. J.*, 2016, **284**, 260–269.

152 Z. Cui, S. Meng, Y. Yi, A. Jafarzadeh, S. Li, E. C. Neyts, Y. Hao, L. Li, X. Zhang and X. Wang, *ACS Catal.*, 2022, **12**, 1326–1337.

153 D. Mignard, M. Sahibzada, J. Duthie and H. Whittington, *Int. J. Hydrogen Energy*, 2003, **28**, 455–464.

154 S. Kwon, H. Yang, Y. Yu, Y. Choi, N. Kim, G. H. Kim, K. C. Ko and K. Na, *Appl. Catal. B Environ.*, 2023, **339**, 123120.

155 J. Niu, H. Liu, Y. Jin, B. Fan, W. Qi and J. Ran, *Int. J. Hydrogen Energy*, 2022, **47**, 9183–9200.

156 J. Zhong, X. Yang, Z. Wu, B. Liang, Y. Huang and T. Zhang, *Chem. Soc. Rev.*, 2020, **49**, 1385–1413.

157 M. D. Porosoff, B. Yan and J. G. Chen, *Energy Environ. Sci.*, 2016, **9**, 62–73.

158 H. Sugiyama, M. Miyazaki, M. Sasase, M. Kitano and H. Hosono, *J. Am. Chem. Soc.*, 2023, **145**, 9410–9416.

159 F. Cannizzaro, E. J. Hensen and I. A. Filot, *ACS Catal.*, 2023, **13**, 1875–1892.

160 H. Zhang, D. Mao, J. Zhang and D. Wu, *Chem. Eng. J.*, 2023, **452**, 139144.

161 J. Wu, M. Saito, M. Takeuchi and T. Watanabe, *Appl. Catal. A*, 2001, **218**, 235–240.

162 M. B. Fichtl, D. Schlereth, N. Jacobsen, I. Kasatkina, J. Schumann, M. Behrens, R. Schlögl and O. Hinrichsen, *Appl. Catal. A*, 2015, **502**, 262–270.

163 O. Martin and J. Pérez-Ramírez, *Catal. Sci. Technol.*, 2013, **3**, 3343–3352.

164 T. P. Araújo, J. Morales-Vidal, G. Giannakakis, C. Mondelli, H. Eliasson, R. Erni, J. A. Stewart, S. Mitchell, N. López and J. Pérez-Ramírez, *Angew. Chem. Int. Ed.*, 2023, **62**, e202306563.

165 Y. Wang, B. Yang, B. Gao, L. Li, Y. Zhou, Y. Zhang, T. Ishihara and L. Guo, *Appl. Catal. A*, 2023, **665**, 119374.

166 J. Díez-Ramírez, J. L. Valverde, P. Sánchez and F. Dorado, *Catal. Lett.*, 2016, **146**, 373–382.

167 A. S. Malik, S. F. Zaman, A. A. Al-Zahrani, M. A. Daous, H. Driss and L. A. Petrov, *Appl. Catal. A*, 2018, **560**, 42–53.

168 O. A. Ojelade, S. F. Zaman, M. A. Daous, A. A. Al-Zahrani, A. S. Malik, H. Driss, G. Shterk and J. Gascon, *Appl. Catal. A*, 2019, **584**, 117185.



169 L. Oar-Arteta, A. Remiro, F. Epron, N. Bion, A. T. Aguayo, J. Bilbao and A. G. Gayubo, *Ind. Eng. Chem. Res.*, 2016, **55**, 3546–3555.

170 S. Ghoshal and P. Sarkar, *J. Phys. Chem. C*, 2024, **128**, 2392–2405.

171 F. Lyu, M. Cao, A. Mabsud and Q. Zhang, *J. Mater. Chem. A*, 2020, **8**, 15445–15457.

172 Z. Seh, J. Kibsgaard, C. Dickens, I. Chorkendorff, J. Nørskov and T. Jaramillo, *Science*, 2017, **355**, 6321.

173 X. Liu, Q. Gu, Y. Zhang, X. Xu, H. Wang, Z. Sun, L. Cao, Q. Sun, L. Xu and L. Wang, *J. Am. Chem. Soc.*, 2023, **145**, 6702–6709.

174 X. Li, M. Song, Y. Zhou, P. Zhou, D. Xu, T. Liu and X. Hong, *ChemCatChem*, 2024, e202301577.

175 S. Natesakhawat, J. W. Lekse, J. P. Baltrus, P. R. Ohodnicki Jr, B. H. Howard, X. Deng and C. Matranga, *ACS Catal.*, 2012, **2**, 1667–1676.

176 M. Abdelgaid and G. Mpourmpakis, *ACS Catal.*, 2022, **12**, 4268–4289.

177 F. Hu, R. Ye, Z.-H. Lu, R. Zhang and G. Feng, *Energy Fuels*, 2021, **36**, 156–169.

178 R. Singh, K. Kundu and K. K. Pant, *Chem. Eng. J.*, 2024, **479**, 147783.

179 K. Liu, J. Niu, Y. Bai, J. Qi, L. Han, N. Zhu and L. Yan, *J. Colloid Interface Sci.*, 2025, **683**, 1030–1040.

180 A. M. Bahmanpour, M. Signorile and O. Kröcher, *Appl. Catal., B*, 2021, **295**, 120319.

181 N. M. Martin, P. Velin, M. Skoglundh, M. Bauer and P.-A. Carlsson, *Catal. Sci. Technol.*, 2017, **7**, 1086–1094.

182 M. González-Castaño, P. Tarifa, A. Monzon and H. Arellano-Garcia, in *Circular Economy Processes for CO<sub>2</sub> Capture and Utilization*, Elsevier, 2024, pp. 307–323.

183 Y. He, F. H. Müller, R. Palkovits, F. Zeng and C. Mebrahtu, *Appl. Catal. B Environ.*, 2024, 123663.

184 J. Guo, L. Wang, Z. Jin, Z. Liu, H. Hao, J. Gong and Z. Wang, *Chem. Eng. J.*, 2024, 155160.

185 L. Guo, J. Zhou, F. Liu, X. Meng, Y. Ma, F. Hao, Y. Xiong and Z. Fan, *ACS Nano*, 2024, **18**, 9823–9851.

186 X. Dong, X. Li, H. Tan, J. Zhu, G. Wang, S. Wang, W. Xie, T. Zhan and V. Polshettiwar, *Mol. Catal.*, 2023, **547**, 113369.

187 J. Fan, H. Du, Y. Zhao, Q. Wang, Y. Liu, D. Li and J. Feng, *ACS Catal.*, 2020, **10**, 13560–13583.

188 S. Jiao, X. Fu and H. Huang, *Adv. Funct. Mater.*, 2022, **32**, 2107651.

189 H. Chen, Q. Wu, Y. Wang, Q. Zhao, X. Ai, Y. Shen and X. Zou, *ChemComm*, 2022, **58**, 7730–7740.

190 M. Wang, Y. Xiang, Y. Lin, Y. Sun, Z.-z. Zhu, S. Wu and X. Cao, *J. Mater. Chem. A*, 2024, **12**, 31902–31913.

191 W. Li, H. Wang, X. Zheng, L. Ricardez-Sandoval, Q. Wu and G. Bai, *Chem. Eng. J.*, 2023, **453**, 139779.

192 K.-Q. Lu, Y.-H. Li, F. Zhang, M.-Y. Qi, X. Chen, Z.-R. Tang, Y. M. Yamada, M. Anpo, M. Conte and Y.-J. Xu, *Nat. Commun.*, 2020, **11**, 5181.

193 Z. Chen, A. Huang, K. Yu, T. Cui, Z. Zhuang, S. Liu, J. Li, R. Tu, K. Sun and X. Tan, *Energy Environ. Sci.*, 2021, **14**, 3430–3437.

194 L. Fu, R. Wang, C. Zhao, J. Huo, C. He, K.-H. Kim and W. Zhang, *Chem. Eng. J.*, 2021, **414**, 128857.

195 J. Klankermayer, S. Wesselbaum, K. Beydoun and W. Leitner, *Angew. Chem. Int. Ed.*, 2016, **55**, 7296–7343.

196 U. B. Kim, D. J. Jung, H. J. Jeon, K. Rathwell and S.-g. Lee, *Chem. Rev.*, 2020, **120**, 13382–13433.

197 J. Xu, X. Su, X. Liu, X. Pan, G. Pei, Y. Huang, X. Wang, T. Zhang and H. Geng, *Appl. Catal., A*, 2016, **514**, 51–59.

198 L. E. Briand, A. M. Hirt and I. E. Wachs, *J. Catal.*, 2001, **202**, 268–278.

199 Z. Liu, F. Huang, M. Peng, Y. Chen, X. Cai, L. Wang, Z. Hu, X. Wen, N. Wang and D. Xiao, *Nat. Commun.*, 2021, **12**, 6194.

200 J. Liang, F. Ma, S. Hwang, X. Wang, J. Sokolowski, Q. Li, G. Wu and D. Su, *Joule*, 2019, **3**, 956–991.

201 M. A. Z. G. Sial, M. A. U. Din and X. Wang, *Chem. Soc. Rev.*, 2018, **47**, 6175–6200.

202 W. Xiao, W. Lei, M. Gong, H. L. Xin and D. Wang, *ACS Catal.*, 2018, **8**, 3237–3256.

203 X. Wang, J. Pan, H. Wei, W. Li, J. Zhao and Z. Hu, *J. Phys. Chem. C*, 2022, **126**, 1761–1769.

204 Q. Shao, P. Wang, T. Zhu and X. Huang, *Acc. Chem. Res.*, 2019, **52**, 3384–3396.

205 P. Yang, J. Zheng, Y. Xu, Q. Zhang and L. Jiang, *Adv. Mater.*, 2016, **28**, 10508–10517.

206 S. W. Lee, M. L. Luna, N. Berdunov, W. Wan, S. Kunze, S. Shaikhutdinov and B. R. Cuenya, *Nat. Commun.*, 2023, **14**, 4649.

207 H.-H. Wang, J.-F. Zhang, Z.-L. Chen, M.-M. Zhang, X.-P. Han, C. Zhong, Y.-D. Deng and W.-B. Hu, *Rare Met.*, 2019, **38**, 115–121.

208 J. Zhu, P. Wang, X. Zhang, G. Zhang, R. Li, W. Li, T. P. Senftle, W. Liu, J. Wang and Y. Wang, *Sci. Adv.*, 2022, **8**, eabm3629.

209 B. Gao, Z. Wen, Y. Wang, D. Chen, B. Yang, T. Ishihara and L. Guo, *ChemCatChem*, 2024, **16**, e202400814.

210 J. Zhu, S. Shaikhutdinov and B. R. Cuenya, *Chem. Sci.*, 2025, **16**, 1071–1092.

211 P. Schwiderowski, H. Ruland and M. Muhler, *Curr. Opin. Green Sustainable Chem.*, 2022, **38**, 100688.

212 N. Onishi and Y. Himeda, *Acc. Chem. Res.*, 2024, **57**, 2816–2825.

213 S. Navarro-Jaén, M. Virginie, J. Bonin, M. Robert, R. Wojcieszak and A. Y. Khodakov, *Nat. Rev. Chem.*, 2021, **5**, 564–579.

214 M. A. Adnan and M. G. Kibria, *Appl. Energy*, 2020, **278**, 115614.

215 A. Álvarez, M. Borges, J. J. Corral-Pérez, J. G. Olcina, L. Hu, D. Cornu, R. Huang, D. Stoian and A. Urakawa, *ChemPhysChem*, 2017, **18**, 3135–3141.

216 J. O. Edwards and R. G. Pearson, *J. Am. Chem. Soc.*, 1962, **84**, 16–24.

217 D. Qin, Y. Zhou, W. Wang, C. Zhang, G. Zeng, D. Huang, L. Wang, H. Wang, Y. Yang and L. Lei, *J. Mater. Chem. A*, 2020, **8**, 19156–19195.



218 H. Ahouari, A. Soualah, A. Le Valant, L. Pinard, P. Magnoux and Y. Pouilloux, *catalysis, React. Kinet. Mech. Catal.*, 2013, **110**, 131–145.

219 S. L. Suib, *New and Future Developments in Catalysis: Activation of Carbon Dioxide*, Newnes, 2013.

220 M. Aresta, A. Dibenedetto and E. Quaranta, *J. Catal.*, 2016, **343**, 2–45.

221 K. Stangeland, H. Li and Z. Yu, *Ind. Eng. Chem. Res.*, 2018, **57**, 4081–4094.

222 R. Schlögl, *Chemical Energy Storage*, de Gruyter, Berlin, 2013.

223 J. Ma, N. Sun, X. Zhang, N. Zhao, F. Xiao, W. Wei and Y. Sun, *Catal. Today*, 2009, **148**, 221–231.

224 H.-J. Yin, J.-H. Zhou and Y.-W. Zhang, *Inorg. Chem. Front.*, 2019, **6**, 2582–2618.

225 S. Kattel, P. J. Ramírez, J. G. Chen, J. A. Rodriguez and P. Liu, *Science*, 2017, **355**, 1296–1299.

226 S. Kattel, P. Liu and J. G. Chen, *J. Am. Chem. Soc.*, 2017, **139**, 9739–9754.

227 J. Wang, G. Li, Z. Li, C. Tang, Z. Feng, H. An, H. Liu, T. Liu and C. Li, *Sci. Adv.*, 2017, **3**, e1701290.

228 X. Su, X.-F. Yang, Y. Huang, B. Liu and T. Zhang, *Acc. Chem. Res.*, 2018, **52**, 656–664.

229 D. Xu, P. Wu and B. y. Yang, *Catal. Sci. Technol.*, 2020, **10**, 3346–3352.

230 G. Yan, Z. Gao, M. Zhao, W. Yang and X. Ding, *Appl. Surf. Sci.*, 2020, **517**, 146200.

231 J. Ye, C.-j. Liu, D. Mei and Q. Ge, *J. Catal.*, 2014, **317**, 44–53.

232 C. Panzone, R. Philippe, C. Nikitine, A. Bengaouer, A. Chappaz and P. Fongarland, *Ind. Eng. Chem. Res.*, 2022, **61**, 4514–4533.

233 Q.-J. Hong and Z.-P. Liu, *Surf. Sci.*, 2010, **604**, 1869–1876.

234 D. Kopac, M. Hus, M. Ogrizek and B. Likozar, *J. Phys. Chem. C*, 2017, **121**, 17941–17949.

235 Q.-L. Tang, Q.-J. Hong and Z.-P. Liu, *J. Catal.*, 2009, **263**, 114–122.

236 Y. Yang, J. Evans, J. A. Rodriguez, M. G. White and P. Liu, *Phys. Chem. Chem. Phys.*, 2010, **12**, 9909–9917.

237 C. Gilbert, L. Gilbey, A. Caragheorgheopol, F. Savonea, D. B. Jackson, B. Onida, E. Garrone and R. Luque, *J. Mater. Chem.*, 2005, **15**, 3946–3951.

238 Q. Tang, Z. Shen, C. K. Russell and M. Fan, *J. Phys. Chem. C*, 2018, **122**, 315–330.

239 W. Liu, D. Wang and J. Ren, *Appl. Surf. Sci.*, 2020, **505**, 144528.

240 Y. Kim, T. S. B. Trung, S. Yang, S. Kim and H. Lee, *ACS Catal.*, 2016, **6**, 1037–1044.

241 Y. Zhuang, R. Currie, K. B. McAuley and D. S. Simakov, *Appl. Catal., A*, 2019, **575**, 74–86.

242 F. Sha, Z. Han, S. Tang, J. Wang and C. Li, *ChemSusChem*, 2020, **13**, 6160–6181.

243 T. Fujitani and J. Nakamura, *Catal. Lett.*, 1998, **56**, 119–124.

244 Y. Choi, K. Futagami, T. Fujitani and J. Nakamura, *Appl. Catal., A*, 2001, **208**, 163–167.

245 S. E. Collins, M. A. Baltanas and A. L. Bonivardi, *J. Catal.*, 2004, **226**, 410–421.

246 F. Liao, X.-P. Wu, J. Zheng, M.-J. Li, Z. Zeng, X. Hong, A. Kroner, Y. Yuan, X.-Q. Gong and S. C. E. Tsang, *Catal. Sci. Technol.*, 2016, **6**, 7698–7702.

247 M. Huš, D. Kopač, N. S. Štefančič, D. L. Jurković, V. D. Dasireddy and B. Likozar, *Catal. Sci. Technol.*, 2017, **7**, 5900–5913.

248 S. G. Neophytides, A. J. Marchi and G. F. Froment, *Appl. Catal., A*, 1992, **86**, 45–64.

249 E. L. Kunkes, F. Studt, F. Abild-Pedersen, R. Schlögl and M. Behrens, *J. Catal.*, 2015, **328**, 43–48.

250 Z. Zhang, Y. Zheng, L. Qian, D. Luo, H. Dou, G. Wen, A. Yu and Z. Chen, *Adv. Mater.*, 2022, 2201547.

251 D. L. Chiavassa, S. E. Collins, A. L. Bonivardi and M. A. Baltanás, *Chem. Eng. J.*, 2009, **150**, 204–212.

252 L. Grabow and M. Mavrikakis, *ACS Catal.*, 2011, **1**, 365–384.

253 M. Behrens, F. Studt, I. Kasatkin, S. Kühl, M. Hävecker, F. Abild-Pedersen, S. Zander, F. Girsdsies, P. Kurr and B.-L. Kniep, *Science*, 2012, **336**, 893–897.

254 J. A. Rodriguez, J. Evans, L. Feria, A. B. Vidal, P. Liu, K. Nakamura and F. Illas, *J. Catal.*, 2013, **307**, 162–169.

255 J. Artz, T. E. Müller, K. Thenert, J. Kleinekorte, R. Meys, A. Sternberg, A. Bardow and W. Leitner, *Chem. Rev.*, 2018, **118**, 434–504.

256 S. Roy, A. Cherevotan and S. C. Peter, *ACS Energy Lett.*, 2018, **3**, 1938–1966.

257 X. Yang, S. Kattel, S. D. Senanayake, J. A. Boscoboinik, X. Nie, J. Graciani, J. A. Rodriguez, P. Liu, D. J. Stacchiola and J. G. Chen, *J. Am. Chem. Soc.*, 2015, **137**, 10104–10107.

258 Y.-F. Zhao, Y. Yang, C. Mims, C. H. Peden, J. Li and D. Mei, *J. Catal.*, 2011, **281**, 199–211.

259 C. Liu and P. Liu, *ACS Catal.*, 2015, **5**, 1004–1012.

260 S. Kattel, B. Yan, Y. Yang, J. G. Chen and P. Liu, *J. Am. Chem. Soc.*, 2016, **138**, 12440–12450.

261 Q. Tang, Z. Shen, L. Huang, T. He, H. Adidharma, A. G. Russell and M. Fan, *Phys. Chem. Chem. Phys.*, 2017, **19**, 18539–18555.

262 N. Pasupulety, H. Driss, Y. A. Alhamed, A. A. Alzahrani, M. A. Daous and L. Petrov, *Appl. Catal., A*, 2015, **504**, 308–318.

263 P. Banoth, C. Kandula and P. Kollu, in *Noble Metal-free Electrocatalysts: New Trends in Electrocatalysts for Energy Applications*, vol. 2, ACS Publications, 2022, pp. 1–37.

264 X.-F. Yang, A. Wang, B. Qiao, J. Li, J. Liu and T. Zhang, *Acc. Chem. Res.*, 2013, **46**, 1740–1748.

265 M. Humayun, M. Israr, A. Khan and M. Bououdina, *Nano Energy*, 2023, **113**, 108570.

266 P. Sharma, S. Kumar, O. Tomanec, M. Petr, J. Zhu Chen, J. T. Miller, R. S. Varma, M. B. Gawande and R. Zbořil, *Small*, 2021, **17**, 2006478.

267 J. Zhong, X. Yang, Z. Wu, B. Liang, Y. Huang and T. Zhang, *Chem. Soc. Rev.*, 2020, **49**, 1385–1413.

268 J. Frost, *Nature*, 1988, **334**, 577–580.

269 P. L. Hansen, J. B. Wagner, S. Helveg, J. R. Rostrup-Nielsen, B. S. Clausen and H. Topsøe, *Science*, 2002, **295**, 2053–2055.

270 G. A. Olah, A. Goeppert and G. S. Prakash, *Beyond Oil and Gas: the Methanol Economy*, John Wiley & Sons, 2011.



271 C. T. Campbell and C. H. Peden, *Science*, 2005, **309**, 713–714.

272 M. Zabilskiy, V. L. Sushkevich, D. Palagin, M. A. Newton, F. Krumeich and J. A. van Bokhoven, *Nat. Commun.*, 2020, **11**, 2409.

273 Z. Zhang, C. Mao, D. M. Meira, P. N. Duchesne, A. A. Tountas, Z. Li, C. Qiu, S. Tang, R. Song and X. Ding, *Nat. Commun.*, 2022, **13**, 1512.

274 J. Graciani, K. Mudiyanselage, F. Xu, A. E. Baber, J. Evans, S. D. Senanayake, D. J. Stacchiola, P. Liu, J. Hrbek and J. F. Sanz, *Science*, 2014, **345**, 546–550.

275 P. Gao, S. Li, X. Bu, S. Dang, Z. Liu, H. Wang, L. Zhong, M. Qiu, C. Yang and J. Cai, *Nat. Chem.*, 2017, **9**, 1019–1024.

276 B. Liu, C. Li, G. Zhang, X. Yao, S. S. Chuang and Z. Li, *ACS Catal.*, 2018, **8**, 10446–10456.

277 K. Li and J. G. Chen, *ACS Catal.*, 2019, **9**, 7840–7861.

278 G. Wang, D. Mao, X. Guo and J. Yu, *Int. J. Hydrogen Energy*, 2019, **44**, 4197–4207.

279 B. Min, A. Santra and D. Goodman, *Catal. Today*, 2003, **85**, 113–124.

280 F. Chen, C. Kreyenschulte, J. r. Radnik, H. Lund, A.-E. Surkus, K. Junge and M. Beller, *ACS Catal.*, 2017, **7**, 1526–1532.

281 R. P. Mogorosi, N. Fischer, M. Claeys and E. van Steen, *J. Catal.*, 2012, **289**, 140–150.

282 R. Takahashi, S. Sato, T. Sodesawa, M. Yoshida and S. Tomiyama, *Appl. Catal., A*, 2004, **273**, 211–215.

283 A. T. Aguayo, J. Erefa, D. Mier, J. M. Arandes, M. Olazar and J. Bilbao, *Ind. Eng. Chem. Res.*, 2007, **46**, 5522–5530.

284 J. Díez-Ramírez, P. Sanchez, A. Rodriguez-Gomez, J. L. Valverde and F. Dorado, *Ind. Eng. Chem. Res.*, 2016, **55**, 3556–3567.

285 V. I. Bogdan, Y. A. Pokusaeva, A. E. Koklin, S. V. Savilov, S. A. Chernyak, V. V. Lunin and L. M. Kustov, *Energy Technol.*, 2019, **7**, 1900174.

286 J. A. Rodriguez, P. Liu, D. J. Stacchiola, S. D. Senanayake, M. G. White and J. G. Chen, *ACS Catal.*, 2015, **5**, 6696–6706.

287 H. Sakurai, S. Tsubota and M. Haruta, *Appl. Catal., A*, 1993, **102**, 125–136.

288 F. Liao, Z. Zeng, C. Eley, Q. Lu, X. Hong and S. C. E. Tsang, *Angew. Chem., Int. Ed.*, 2012, **24**, 5832–5836.

289 I. A. Da Silva and C. J. Mota, *Front. Energy Res.*, 2019, **7**, 49.

290 I. U. Din, M. S. Shaharun, D. Subbarao, A. Naeem and F. Hussain, *Catal. Today*, 2016, **259**, 303–311.

291 Y. Wang, S. Kattel, W. Gao, K. Li, P. Liu, J. G. Chen and H. Wang, *Nat. Commun.*, 2019, **10**, 1166.

292 M. Zabilskiy, V. L. Sushkevich, D. Palagin, M. A. Newton, F. Krumeich and J. A. van Bokhoven, *Nat. Commun.*, 2020, **11**, 2409.

293 L. Wang, Y. Dong, T. Yan, Z. Hu, F. M. Ali, D. M. Meira, P. N. Duchesne, J. Y. Y. Loh, C. Qiu and E. E. Storey, *Nat. Commun.*, 2020, **11**, 2432.

294 A. e. Prasnikar, A. Pavlisic, F. Ruiz-Zepeda, J. Kovac and B. Likozar, *Ind. Eng. Chem. Res.*, 2019, **58**, 13021–13029.

295 A. H. Leung, A. García-Treco, A. Phanopoulos, A. Regoutz, M. E. Schuster, S. D. Pike, M. S. Shaffer and C. K. Williams, *J. Mater. Chem. A*, 2020, **8**, 11282–11291.

296 F. Studt, M. Behrens, E. L. Kunkes, N. Thomas, S. Zander, A. Tarasov, J. Schumann, E. Frei, J. B. Varley and F. Abild-Pedersen, *ChemCatChem*, 2015, **7**, 1105–1111.

297 S. G. Jadhav, P. D. Vaidya, B. M. Bhanage and J. B. Joshi, *Chem. Eng. Res. Des.*, 2014, **92**, 2557–2567.

298 O. A. Ojelade and S. F. Zaman, *Catal. Surv. Asia*, 2020, **24**, 11–37.

299 S. G. Jadhav, P. D. Vaidya, B. M. Bhanage and J. B. Joshi, *Chem. Eng. Res. Des.*, 2014, **92**, 2557–2567.

300 J. Schittkowski, H. Ruland, D. Laudenschleger, K. Girod, K. Kähler, S. Kaluza, M. Muhler and R. Schlögl, *Chem. Ing. Tech.*, 2018, **90**, 1419–1429.

301 X.-M. Liu, G. Lu, Z.-F. Yan and J. Beltramini, *Ind. Eng. Chem. Res.*, 2003, **42**, 6518–6530.

302 T. T. N. Vu, A. Desgagnés and M. C. Iliuta, *Appl. Catal., A*, 2021, **617**, 118119.

303 X. Nie, X. Jiang, H. Wang, W. Luo, M. J. Janik, Y. Chen, X. Guo and C. Song, *ACS Catal.*, 2018, **8**, 4873–4892.

304 A. S. Malik, S. F. Zaman, A. A. Al-Zahrani, M. A. Daous, H. Driss and L. A. Petrov, *Catal. Today*, 2020, **357**, 573–582.

305 B. Hu, Y. Yin, G. Liu, S. Chen, X. Hong and S. C. E. Tsang, *J. Catal.*, 2018, **359**, 17–26.

306 A. Ota, E. L. Kunkes, I. Kasatkin, E. Groppo, D. Ferri, B. Poceiro, R. M. N. Yerga and M. Behrens, *J. Catal.*, 2012, **293**, 27–38.

307 M. Bowker, N. Lawes, I. Gow, J. Hayward, J. R. Esquius, N. Richards, L. R. Smith, T. J. Slater, T. E. Davies and N. F. Dummer, *ACS Catal.*, 2022, **12**, 5371–5379.

308 S. Kanuri, S. Roy, C. Chakraborty, S. P. Datta, S. A. Singh and S. Dinda, *Int. J. Energy Res.*, 2022, **46**, 5503–5522.

309 Y. Zeng, Y. Chen, Y. Wu, D. Wang, X. Liu and L. Li, *Organometallics*, 2022, **41**, 2001–2010.

310 S. Bai, Q. Shao, P. Wang, Q. Dai, X. Wang and X. Huang, *J. Am. Chem. Soc.*, 2017, **139**, 6827–6830.

311 R. Manrique, J. Rodríguez-Pereira, S. A. Rincón-Ortiz, J. J. Bravo-Suárez, V. G. Baldovino-Medrano, R. Jiménez and A. Karelovic, *Catal. Sci. Technol.*, 2020, **10**, 6644–6658.

312 A. Erdöhelyi, M. Pásztor and F. Solymosi, *J. Catal.*, 1986, **98**, 166–177.

313 J. Wang, G. Zhang, J. Zhu, X. Zhang, F. Ding, A. Zhang, X. Guo and C. Song, *ACS Catal.*, 2021, **11**, 1406–1423.

314 H. Jiang, J. Lin, X. Wu, W. Wang, Y. Chen and M. Zhang, *J. CO<sub>2</sub> Util.*, 2020, **36**, 33–39.

315 X.-L. Liang, X. Dong, G.-D. Lin and H.-B. Zhang, *Appl. Catal., B*, 2009, **88**, 315–322.

316 I. U. Din, M. S. Shaharun, D. Subbarao, A. Naeem and F. Hussain, *Catal. Today*, 2016, **259**, 303–311.

317 M. Chatterjee, T. Ishizaka and H. Kawanami, in *Advances in CO<sub>2</sub> Capture, Sequestration, and Conversion*, ACS Publications, 2015, pp. 191–250.

318 N. Iwasa, H. Suzuki, M. Terashita, M. Arai and N. Takezawa, *Catal. Lett.*, 2004, **96**, 75–78.

319 J. Xu, X. Su, X. Liu, X. Pan, G. Pei, Y. Huang, X. Wang, T. Zhang and H. Geng, *Appl. Catal.*, 2016, **514**, 51–59.

320 H. Bahruji, M. Bowker, G. Hutchings, N. Dimitratos, P. Wells, E. Gibson, W. Jones, C. Brookes, D. Morgan and G. Lalev, *J. Catal.*, 2016, **343**, 133–146.



321 H. Bahruji, M. Bowker, W. Jones, J. Hayward, J. R. Esquius, D. Morgan and G. Hutchings, *Faraday Discuss.*, 2017, **197**, 309–324.

322 F. Liao, X.-P. Wu, J. Zheng, M. M.-J. Li, A. Kroner, Z. Zeng, X. Hong, Y. Yuan, X.-Q. Gong and S. C. E. Tsang, *Green Chem.*, 2017, **19**, 270–280.

323 A. S. Malik, S. F. Zaman, A. A. Al-Zahrani, M. A. Daous, H. Driss and L. A. Petrov, *Catal.*, 2020, **357**, 573–582.

324 J. Diez-Ramirez, P. Sanchez, A. Rodriguez-Gomez, J. L. Valverde and F. Dorado, *Ind. Eng. Chem. Res.*, 2016, **55**, 3556–3567.

325 C. Quilis, N. Mota, B. Pawelec, E. Millan and R. M. N. Yerga, *Appl. Catal., B*, 2023, **321**, 122064.

326 X. Yao, S. Yuan, C. Li, L. Wang, X. Yu, P. Tian and S.-t. Tu, *Fuel*, 2024, **358**, 130133.

327 X. Jiang, X. Wang, X. Nie, N. Koizumi, X. Guo and C. Song, *Catal.*, 2018, **316**, 62–70.

328 X. Jiang, X. Nie, X. Wang, H. Wang, N. Koizumi, Y. Chen, X. Guo and C. Song, *J. Catal.*, 2019, **369**, 21–32.

329 F. Lin, X. Jiang, N. Boreriboon, Z. Wang, C. Song and K. Cen, *Appl. Catal.*, 2019, **585**, 117210.

330 T. Fujitani, M. Saito, Y. Kanai, T. Watanabe, J. Nakamura and T. Uchijima, *Appl. Catal.*, 1995, **125**, L199–L202.

331 S. E. Collins, M. A. Baltanás, J. L. G. Fierro and A. L. Bonivardi, *J. Catal.*, 2002, **211**, 252–264.

332 L. Li, B. Zhang, E. Kunkes, K. Föttinger, M. Armbrüster, D. S. Su, W. Wei, R. Schlögl and M. Behrens, *ChemCatChem*, 2012, **4**, 1764–1775.

333 E. M. Fiordaliso, I. Sharafutdinov, H. W. Carvalho, J.-D. Grunwaldt, T. W. Hansen, I. Chorkendorff, J. B. Wagner and C. D. Damsgaard, *ACS Catal.*, 2015, **5**, 5827–5836.

334 X. Zhou, J. Qu, F. Xu, J. Hu, J. S. Foord, Z. Zeng, X. Hong and S. C. E. Tsang, *Chem. Commun.*, 2013, **49**, 1747–1749.

335 A. s. García-Treco, E. R. White, A. Regoutz, D. J. Payne, M. S. Shaffer and C. K. Williams, *ACS Catal.*, 2017, **7**, 1186–1196.

336 N. Lawes, N. F. Dummer, S. Fagan, O. Wielgosz, I. E. Gow, L. R. Smith, T. J. Slater, T. E. Davies, K. J. Aggett and D. J. Morgan, *Appl. Catal., A*, 2024, **679**, 119735.

337 A. García-Treco, A. Regoutz, E. R. White, D. J. Payne, M. S. Shaffer and C. K. Williams, *Appl. Catal., B*, 2018, **220**, 9–18.

338 J. L. Snider, V. Streibel, M. A. Hubert, T. S. Choksi, E. Valle, D. C. Upham, J. Schumann, M. S. Duyar, A. Gallo and F. Abild-Pedersen, *ACS Catal.*, 2019, **9**, 3399–3412.

339 N. Rui, Z. Wang, K. Sun, J. Ye, Q. Ge and C.-J. Liu, *Appl. Catal., B*, 2017, **218**, 488–497.

340 T. Pinheiro Araújo, C. Mondelli, M. Agrachev, T. Zou, P. O. Willi, K. M. Engel, R. N. Grass, W. J. Stark, O. V. Safonova and G. Jeschke, *Nat. Commun.*, 2022, **13**, 1–12.

341 Z. Cai, J. Dai, W. Li, K. B. Tan, Z. Huang, G. Zhan, J. Huang and Q. Li, *ACS Catal.*, 2020, **10**, 13275–13289.

342 H. Jiang, J. Lin, X. Wu, W. Wang, Y. Chen and M. Zhang, *J. CO<sub>2</sub> Util.*, 2020, **36**, 33–39.

343 J. Wu, B. Lu, S. Yang, J. Huang, W. Wang, R. Dun and Z. Hua, *ChemSusChem*, 2024, e202400543.

344 N. Koizumi, X. Jiang, J. Kugai and C. Song, *Catal.*, 2012, **194**, 16–24.

345 A. Velty and A. Corma, *Chem. Soc. Rev.*, 2023, **52**, 1773–1946.

346 P. Romero-Marimon, J. J. Gutiérrez-Sevillano and S. Calero, *Chem. Mater.*, 2023, **35**, 5222–5231.

347 X.-L. Liang, X. Dong, G.-D. Lin and H.-B. Zhang, *Appl. Catal., B*, 2009, **88**, 315–322.

348 H. Kong, H.-Y. Li, G.-D. Lin and H.-B. Zhang, *Catal. Lett.*, 2011, **141**, 886–894.

349 J. Wang, S.-m. Lu, J. Li and C. Li, *Chem. Commun.*, 2015, **51**, 17615–17618.

350 E. J. Choi, Y. H. Lee, D.-W. Lee, D.-J. Moon and K.-Y. Lee, *Mol. Catal.*, 2017, **434**, 146–153.

351 Y. Yin, B. Hu, X. Li, X. Zhou, X. Hong and G. Liu, *Appl. Catal., B*, 2018, **234**, 143–152.

352 A. Vourros, I. Garagounis, V. Kyriakou, S. Carabineiro, F. Maldonado-Hódar, G. Marnellos and M. Konsolakis, *J. CO<sub>2</sub> Util.*, 2017, **19**, 247–256.

353 Y. Hartadi, D. Widmann and R. J. Behm, *Phys. Chem. Chem. Phys.*, 2016, **18**, 10781–10791.

354 Y. Hartadi, D. Widmann and R. J. Behm, *J. Catal.*, 2016, **333**, 238–250.

355 C. Wu, P. Zhang, Z. Zhang, L. Zhang, G. Yang and B. Han, *ChemCatChem*, 2017, **9**, 3691–3696.

356 X. Yang, S. Kattel, S. D. Senanayake, J. A. Boscoboinik, X. Nie, J. Graciani, J. A. Rodriguez, P. Liu, D. J. Stacchiola and J. G. Chen, *J. Am. Chem. Soc.*, 2015, **137**, 10104–10107.

357 K. Prabhakar Reddy, Y. Tian, P. J. Ramírez, A. Islam, H. Lim, N. Rui, Y. Xie, A. Hunt, I. Waluyo and J. A. Rodriguez, *ACS Catal.*, 2024, **14**, 17148–17158.

358 J. Słoczyński, R. Grabowski, A. Kozłowska, P. Olszewski, J. Stoch, J. Skrzypek and M. Lachowska, *Appl. Catal.*, 2004, **278**, 11–23.

359 R. Grabowski, J. Słoczyński, M. Sliwa, D. Mucha, R. Socha, M. Lachowska and J. Skrzypek, *ACS Catal.*, 2011, **1**, 266–278.

360 A. Wang, J. Li and T. Zhang, *Nat. Rev. Chem.*, 2018, **2**, 65–81.

361 H. Li, L. Wang, Y. Dai, Z. Pu, Z. Lao, Y. Chen, M. Wang, X. Zheng, J. Zhu and W. Zhang, *Nat. Nanotechnol.*, 2018, **13**, 411–417.

362 K. W. Ting, T. Toyao, S. H. Siddiki and K.-i. Shimizu, *ACS Catal.*, 2019, **9**, 3685–3693.

363 Z. Han, C. Tang, J. Wang, L. Li and C. Li, *J. Catal.*, 2021, **394**, 236–244.

364 W. Zhang, L. Wang, H. Liu, Y. Hao, H. Li, M. U. Khan and J. Zeng, *Nano Lett.*, 2017, **17**, 788–793.

365 Y. Yin, B. Hu, X. Li, X. Zhou, X. Hong and G. Liu, *Appl. Catal., B*, 2018, **234**, 143–152.

366 M. S. Frei, C. Mondelli, R. García-Muelas, K. S. Kley, B. Puértolas, N. López, O. V. Safonova, J. A. Stewart, D. Curulla Ferré and J. Pérez-Ramírez, *Nat. Commun.*, 2019, **10**, 3377.

367 T. T. N. Vu, P. Fongarland, L. Vanoye, F. Bornette, G. Postole, A. Desgagnés and M. C. Iliuta, *Ind. Eng. Chem. Res.*, 2022, **61**, 15085–15102.



368 F. Lin, X. Jiang, N. Boreriboon, Z. Wang, C. Song and K. Cen, *Appl. Catal., A*, 2019, **585**, 117210.

369 S. Wang, Q. Li, Y. Xin, S. Hu, X. Guo, Y. Zhang, L. Zhang, B. Chen, W. Zhang and L. Wang, *Nanoscale*, 2023, **15**, 6999–7005.

370 J. Guo, Z. Wang, T. Gao and Z. Wang, *Chem. Eng. J.*, 2024, **483**, 149370.

371 J. Song, S. Liu, C. Yang, G. Wang, H. Tian, Z.-j. Zhao, R. Mu and J. Gong, *Appl. Catal., B*, 2020, **263**, 118367.

372 M. Zabilskiy, V. L. Sushkevich, M. A. Newton, F. Krumeich, M. Nachtegaal and J. A. van Bokhoven, *Angew. Chem. Int. Ed.*, 2021, **133**, 17190–17196.

373 F. Jiang, S. Wang, B. Liu, J. Liu, L. Wang, Y. Xiao, Y. Xu and X. Liu, *ACS Catal.*, 2020, **10**, 11493–11509.

374 A. S. Malik, S. F. Zaman, A. A. Al-Zahrani, M. A. Daous, H. Driss and L. A. Petrov, *Appl. Catal.*, 2018, **560**, 42–53.

375 X. Jiang, N. Koizumi, X. Guo and C. Song, *Appl. Catal., B*, 2015, **170**, 173–185.

376 X.-L. Liang, X. Dong, G.-D. Lin and H.-B. Zhang, *Appl. Catal., B*, 2009, **88**, 315–322.

377 T. Fujitani, M. Saito, Y. Kanai, T. Watanabe, J. Nakamura and T. Uchijima, *Appl. Catal., A*, 1995, **125**, L199–L202.

378 K. Lee, U. Anjum, T. P. Araújo, C. Mondelli, Q. He, S. Furukawa, J. Pérez-Ramírez, S. M. Kozlov and N. Yan, *Appl. Catal., B*, 2022, **304**, 120994.

379 K. Sun, N. Rui, Z. Zhang, Z. Sun, Q. Ge and C.-J. Liu, *Green Chem.*, 2020, **22**, 5059–5066.

380 Z. Han, C. Tang, J. Wang, L. Li and C. Li, *J. Catal.*, 2021, **394**, 236–244.

381 Z. Lu, J. Wang, K. Sun, S. Xiong, Z. Zhang and C.-j. Liu, *GreenChe*, 2022, **3**, 165–170.

382 E. S. Gutterød, A. Lazzarini, T. Fjermestad, G. Kaur, M. Manzoli, S. Bordiga, S. Svelle, K. P. Lillerud, E. Skúlason and S. Øien-Ødegaard, *J. Am. Chem. Soc.*, 2019, **142**, 999–1009.

383 Y. Hartadi, D. Widmann and R. J. Behm, *ChemSusChem*, 2015, **8**, 456–465.

384 L. H. Vieira, L. F. Rasteiro, C. S. Santana, G. L. Catuzo, A. H. da Silva, J. M. Assaf and E. M. Assaf, *ChemCatChem*, 2023, **15**, e202300493.

385 Z. Lu, K. Sun, J. Wang, Z. Zhang and C. Liu, *Catalysts*, 2020, **10**, 1360.

386 A. Rezvani, A. M. Abdel-Mageed, T. Ishida, T. Murayama, M. Parlinska-Wojtan and R. J. r. Behm, *ACS Catal.*, 2020, **10**, 3580–3594.

387 N. Rui, F. Zhang, K. Sun, Z. Liu, W. Xu, E. Stavitski, S. D. Senanayake, J. A. Rodriguez and C.-J. Liu, *ACS Catal.*, 2020, **10**, 11307–11317.

388 M. J. Blom, W. P. van Swaaij, G. Mul and S. R. Kersten, *ACS Catal.*, 2021, **11**, 6883–6891.

389 L. Lu, X. Sun, J. Ma, D. Yang, H. Wu, B. Zhang, J. Zhang and B. Han, *Angew. Chem.*, 2018, **130**, 14345–14349.

390 W. Zhang, Q. Qin, L. Dai, R. Qin, X. Zhao, X. Chen, D. Ou, J. Chen, T. T. Chuong and B. Wu, *Angew. Chem. Int. Ed.*, 2018, **57**, 9475–9479.

391 G. Brisard, A. P. M. Camargo, F. C. Nart and T. Iwasita, *Electrochim. Commun.*, 2001, **3**, 603–607.

392 S. Shironita, K. Karasuda, K. Sato and M. Umeda, *J. Power Sources*, 2013, **240**, 404–410.

393 Q.-L. Tang, Q.-J. Hong and Z.-P. Liu, *J. Catal.*, 2009, **263**, 114–122.

394 D. G. Olson, K. Tsuji and I. Shiraishi, *Fuel Process. Technol.*, 2000, **65**, 393–405.

395 M. Saito, T. Fujitani, M. Takeuchi and T. Watanabe, *Appl. Catal., A*, 1996, **138**, 311–318.

396 M. Mikkelsen, M. Jørgensen and F. C. Krebs, *Energy Environ. Sci.*, 2010, **3**, 43–81.

397 M. Ng, V. Jovic, G. I. Waterhouse and J. Kennedy, *Emerg. Mater. Res.*, 2023, **6**, 1097–1115.

398 X. Cui, S. K. Kær and M. P. Nielsen, *Fuel*, 2022, **307**, 121924.

